Asset Diversification versus Climate Action

Christoph Hambel[a] Holger Kraft[b] Frederick van der Ploeg[c]

Current version: February 24, 2021

Abstract: Asset pricing and climate policy are analyzed in a global economy where consumption goods are produced by both a green and a carbon-intensive sector. We allow for endogenous growth and two types of damages from global warming. It is shown that, initially, the desire to diversify assets complements the attempt to mitigate economic damages from climate change. In the longer run, however, a trade-off between diversification and climate action emerges. We derive the optimal carbon price, the equilibrium risk-free rate, and risk premia. Climate disasters, which are more likely to occur sooner as temperature rises, significantly increase risk premia.

Keywords: decarbonization, diversification, carbon price, asset prices, green assets, disaster risk

JEL subject codes: D81, G01, G12, Q5, Q54

[a] Faculty of Economics and Business Administration, Goethe University, Theodor-W.-Adorno-Platz 3, 60323 Frankfurt am Main, Germany. Phone: +49 (0) 69 798 33687.
E-mail: christoph.hambel@finance.uni-frankfurt.de

[b] Faculty of Economics and Business Administration, Goethe University, Theodor-W.-Adorno-Platz 3, 60323 Frankfurt am Main, Germany. Phone: +49 (0) 69 798 33699.
E-mail: holgerkraft@finance.uni-frankfurt.de

[c] University of Oxford, Department of Economics, OXCARRE, Manor Road Building, Oxford OX1 3UQ, U.K. Phone: +44 (0) 1865 281285.
E-mail: rick.vanderploeg@economics.ox.ac.uk. Also affiliated with ASE, University of Amsterdam, P.O. Box 15551, 1001 NB Amsterdam, the Netherlands

We thank Daniel Andrei, Patrick Bolton, Stavros Panageas, Armon Rezai, Eduardo Schwartz, Frank Venmans, and the participants of the Finance seminar at McGill, the European Finance Association (EFA) Meeting 2020, the European Economics Association (EEA) Meeting 2020, the SURED Meeting 2020, the EAERE Meeting 2020, the EBI Global Annual Conference 2020 for helpful comments and suggestions. All remaining errors are our own. Christoph Hambel and Holger Kraft gratefully acknowledge financial support by Deutsche Forschungsgemeinschaft (DFG).

Asset Diversification versus Climate Action

Current version: February 24, 2021

Abstract: Asset pricing and climate policy are analyzed in a global economy where consumption goods are produced by both a green and a carbon-intensive sector. We allow for endogenous growth and two types of damages from global warming. It is shown that, initially, the desire to diversify assets complements the attempt to mitigate economic damages from climate change. In the longer run, however, a trade-off between diversification and climate action emerges. We derive the optimal carbon price, the equilibrium risk-free rate, and risk premia. Climate disasters, which are more likely to occur sooner as temperature rises, significantly increase risk premia.

Keywords: decarbonization, diversification, carbon price, asset prices, green assets, disaster risk

JEL subject codes: D81, G01, G12, Q5, Q54

1 Introduction

Climate change impacts all areas of human life and impacts economic activity.[1] To avoid carbon-dioxide emissions and climate change, emissions-free technologies and renewable energies are developed. Depending on the perceived severity of the consequences of climate change, there are different opinions about how urgent it is to transition to a less carbon-intensive economy. We are interested in the interplay between financial considerations and policies to mitigate climate change and answer two key questions. First, does the financial need to diversify assets hamper or help the fight against climate policy and how does it affect the optimal carbon price? Second, how does climate change and the desire to combat it affects the pricing of green and dirty assets? We highlight that there is a subtle dynamic interdependence between the financial goal to diversify assets in portfolios and the environmental goal to reduce carbon emissions.

Our economic framework is a stochastic macroeconomic growth model with two capital stocks and two energy sources. The green sector takes carbon-free or green energy as input. The dirty sector is carbon-intensive and requires fossil fuel whose combustion leads to carbon emissions. There are two types of capital stocks. Investments and capital reallocation from the dirty to the green capital stock are both subject to adjustment costs. Capital stock accumulation is exposed to diffusive shocks as well as the risk of macroeconomic disasters. Emissions are proportional to fossil fuel use and temperature is driven by cumulative emissions.[2]

We allow for two potential channels for the effect of climate change on economic activity: higher temperature leads to a higher share of damages in pre-damage output as in the seminal DICE-2016R2 model (e.g., Nordhaus 2017). Additionally, higher temperatures might also increase the Poisson risk of a climate-related disaster (e.g. Bansal et al. 2019; Karydas and Xepapadeas 2019).

We first establish the interplay between the intensity of climate action as measured by the size of the optimal carbon price and the economic motive to diversify. Initially, the dirty capital stock dominates the economy and there are two complementary goals: the first one is to mitigate climate change and thus to decarbonize the economy; the second goal is to diversify the economy, which is a purely financial goal. Both goals require policy makers to actively reduce the dirty capital stock. The speed of the transition towards a low-carbon economy is

[1] See, e.g., Scheffers et al. (2019).

[2] See Matthews et al. (2009), Allen et al. (2009), IPCC (2014), van der Ploeg (2018), and Dietz and Venmans (2019), among others, for further references.

thus amplified by the diversification motive. Over time, however, the two goals start to conflict and a trade-off arises. From a diversification perspective, the process should be stopped if there is a balance between green and dirty capital. From an environmental perspective the dirty capital stock should eventually be run down completely. Our various calibrations show, however, that this does not occur unless climate change is extremely severe (relative to the global warming damages in the DICE model (Dynamic Integrated Model of Climate and the Economy) of Nordhaus (2017). Effectively, climate policy drives the dirty capital stock below the fully diversified level, but diversification considerations might prevent the agent from driving it towards zero.

Second, we investigate the interplay between climate change and the pricing of green and dirty assets. We analyze the dynamics of the risk-free rate and risk premia during the transition from a carbon-intensive towards a zero-emissions economy. To separate economic from climate effects, our model includes the risk of macroeconomic disaster shocks as in Barro (2006, 2009) and Pindyck and Wang (2013). Therefore, our model can generate the high equity premium and a low risk-free rate observed in historical data when climate change has had no significant impact on the economy. Taking the effects of climate change into account, our findings for the risk-free rate and risk premia in an economy affected by climate change are different: regardless of how climate change affects the economy, the risk-free interest rate decreases in response to rising temperatures. By contrast, risk premia are only significantly affected if we allow for potential climate disasters for which the probability of them occurring increases with temperature. Without such disasters, the impact on risk premia is modest.

We enrich a well-known asset pricing framework by adding the climate module of an integrated assessment model (IAM). The asset-pricing component involves a model of macroeconomic disasters developed by Barro (2006, 2009) and Wachter (2013), among others. Besides, our representative agent has recursive utility as in Bansal and Yaron (2004) or Pindyck and Wang (2013). We consider an economy with two sectors. If the size of the sectors were exogenous and the effect of climate change is disregarded, then the two-tree model analyzed in Cochrane et al. (2007) arises as special case.

The climate component is related to the literature on integrated assessment models of the economy and the climate. These studies typically have one sector and do not focus on asset pricing. The DICE model is widely used to study optimal carbon abatement and carbon pricing. It combines a Ramsey-type model for capital allocation with deterministic dynamics of emissions,

carbon dioxide and global temperature. The original model is formulated in a deterministic setting (e.g., Nordhaus 1992, 2017). In frameworks with recursive utility, Crost and Traeger (2014), Jensen and Traeger (2014), Ackerman et al. (2013), Bretschger and Vinogradova (2019), van den Bremer and van der Ploeg (2019) analyze versions with stochastic elements. Cai and Lontzek (2019) study a generalization of the DICE model with stochastic growth and the risk of tipping points. Furthermore, there are IAM frameworks that do not fall into the class of DICE models. For instance, Golosov et al. (2014) obtain closed-form solutions in a framework with log utility, Cobb-Douglas production and full depreciation in one discrete time period, and damages that are an exponential function of the atmospheric carbon stock. Traeger (2019) generalizes this setting to recursive preferences and provides a description of the carbon cycle and the climate system and also allows for epistemological uncertainty and anticipated learning.

Few papers combine asset pricing with an integrated assessment model. Barnett et al. (2020) analyze a stochastic one-sector macroeconomic DSGE model of endogenous growth with stochastic economic growth rates and endogenous investments in fossil fuel reserves. They also address the issue of preference-based concerns about ambiguity and model misspecification. Barnett (2020) uses an extended Fama-French 3-factor model to estimate negative climate beta's for brown portfolios and positive climate beta's for green portfolios. He finds a negative climate risk price and also derives optimal climate policy from a DSGE model. While this study in contrast to our paper allows for model uncertainty, we allow for macroeconomic and climatic disasters. Using exogenous climate dynamics, Bansal et al. (2017, 2019) quantify the impact of local temperature on asset prices. They study a global long-run risk model that simultaneously matches the observed temperature and consumption growth dynamics. Furthermore, their model is able to generate a low risk-free interest rate and a high equity premium. Similar results are obtained by Donadelli et al. (2017). Karydas and Xepapadeas (2019) study an economy with two assets, but focus on a Lucas-tree endowment economy where the agent cannot actively control the transition to a low-carbon economy. By contrast, van den Bremer and van der Ploeg (2019) study a one-sector production economy with endogenous climate change and a wide range of economic and climatic uncertainties that generates low risk-adjusted interest rates and a high risk premium. Furthermore, Dietz et al. (2018) address how correlations between future damages and growth affect the discount rate and the carbon price. Finally, Daniel et al. (2019) show in an asset pricing setting that recursive preferences with general resolution of uncertainty about climate change can lead to a declining carbon price.[3]

[3]The feature of a declining carbon price is derived from a binomial tree with a fixed horizon.

Bolton and Kacperczyk (2020b) find using U.S. data that stock with high emissions earn higher returns, even after controlling for size, book to market, momentum and other factors that predict returns. Such carbon risk premia cannot be explained by unexpected profitability or other risk premia. They statistically reject the hypothesis that investors divest from "sin" stocks and also reject the market inefficiency (or carbon alpha) hypothesis, which states that markets under-price carbon risk and thus green stock earn a premium. Bolton and Kacperczyk (2020a) confirm these results for global stock market returns. We also find such a carbon risk premium in our simulations as investors demand compensation for the tipping risk in economic damages which increases with temperature. In future work we want to address the issue of policy transition risk. So long as policy makers are not fully tackling climate change, there is a risk that they will tip into action and step-up climate policy. There is also a probability of a breakthrough in renewable energy or of social tipping with societies abruptly moving from carbon-intensive to carbon-free products. These transition risks lead an additional carbon risk premium. Donadelli et al. (2017) provide evidence that increasing awareness of the global warming challenge has led to increasing carbon risk premia. Bolton and Kacperczyk (2020a) find evidence of rising carbon risk premia for carbon-intensive stocks. The evidence thus suggests that markets have started to price in the climate transition. In future work, we wish to examine how policy transition risk affects the green transition and asset prices.

The remainder of the paper is organized as follows. Section 2 introduces the model setup. Section 3 explains our approach to solving for the social optimum and discusses how the social optimum can be decentralized in the market economy. Section 4 discusses our calibration strategy. Section 5 presents our main results on the relation between the diversification motive and climate action. Section 6 discusses how climate change affects the equilibrium risk-free rate and the risk premia in the economy. Section 7 concludes. The Appendix provides additional material such as proofs and calibration details. It also contains Section F with further simulation results.

2 Model Setup

We present a dynamic two-sector production economy with endogenous growth and production damages resulting from global warming. The green sector uses carbon-free energy as input, whereas the carbon-emitting dirty sector deploys fossil fuel leading to carbon emissions, global

warming and damages to aggregate output. Temperature is driven by cumulative carbon emissions. Energy inputs are unconstrained available. This agent can also reallocate capital from the dirty capital stock to the green capital stock. Both investment and reallocation are costly. The agent has recursive preferences with unit elasticity of intertemporal substitution and a certain coefficient of relative risk aversion.

2.1 Production of Goods

Final goods can be produced in two sectors. The outputs are perfect substitutes. The first is the green sector and the second is the dirty sector. The capital stocks are broad measures which also boost the productivity of labor. Outputs of both sectors are given by the Cobb-Douglas production functions $Y_n = A_n K_n^{\alpha_n} F_n^{\eta_n} (K_n L_n)^{1-\alpha_n-\eta_n} \Lambda_i(T)$, $n \in \{1, 2\}$, where K_n is the capital stock of sector n and L_n is labor supply which is a fixed factor set to unity without loss of generality.[4] The rate of energy use in sector n is denoted by F_n where we refer to F_1 as *green energy* and to F_2 as *fossil fuel use* which causes carbon dioxide emissions. The Cobb-Douglas weights α_n and η_n as well as total factor productivity A_n are non-negative, sector-specific constants, and $\alpha_n + \eta_n < 1$. Here, T denotes global average temperature relative to the beginning of the industrial revolution. So, $T = 0$ is the pre-industrial level of temperature and $T = 2$ is a temperature of two degrees above the pre-industrial level.

The function Λ_n is sector-specific and shows how much output is curbed in response to higher temperatures (e.g., Nordhaus and Sztorc 2013). This is the *first channel* by which climate change influences economic activity. In the sequel, we introduce another channel by which temperature curbs economic activity.[5]

In line with endogenous growth theory, at the aggregate level we have constant returns to scale with respect to capital and energy, i.e.,

$$Y_n = A_n K_n^{1-\eta_n} F_n^{\eta_n} \Lambda_n(T) \tag{2.1}$$

is the output of sector n. In contrast to the long-run exogenous growth rates stemming from labor-augmenting technical progress and population growth in classical growth theory, we have endogenous technical progress captured by the broad measure of capital boosting the efficiency

[4] Our analysis could also be carried out for a CES production function.

[5] This is a temperature dependence of the disaster intensity λ, see (2.2) and (2.3).

of labor and thus ensuring that production at the aggregate level has constant returns to scale with respect to capital and energy. Since the two final goods are perfect substitutes in output, aggregate output is $Y = Y_1 + Y_2$.[6]

2.2 Investments in Green and Dirty Capital

Let I_n be the investment rate in sector n and R the rate at which carbon-emitting capital can be converted into green capital. Investment is subject to quadratic intertemporal adjustment costs. The conversion of dirty into green capital generates quadratic intrasectoral adjustment costs. One dollar of dirty capital can thus be converted into less than one dollar of green capital where the wedge increases in the amount being converted. The depreciation rates of the physical capital stocks are denoted by $\delta_n^k \geq 0$, $n \in \{1, 2\}$.

The capital stock dynamics of the green and dirty sector are then given by[7]

$$\begin{aligned} \mathrm{d}K_1 = &\Big(I_1 - \frac{1}{2}\phi_1 \frac{I_1^2}{K_1} + R - \frac{1}{2}\kappa \frac{R^2}{K_1} - \delta_1^k K_1\Big)\mathrm{d}t + K_1 \sigma_1 \mathrm{d}W_1 \\ &- K_{1-}\Big(\ell_e \mathrm{d}N_e + \ell_c \mathrm{d}N_c\Big), \end{aligned} \tag{2.2}$$

$$\begin{aligned} \mathrm{d}K_2 = &\Big(I_2 - \frac{1}{2}\phi_2 \frac{I_2^2}{K_2} - R - \delta_2^k K_2\Big)\mathrm{d}t + K_2 \sigma_2 \Big(\rho_{12}\mathrm{d}W_1 + \sqrt{1-\rho_{12}^2}\mathrm{d}W_2\Big) \\ &- K_{2-}\Big(\ell_e \mathrm{d}N_e + \ell_c \mathrm{d}N_c\Big), \end{aligned} \tag{2.3}$$

where ϕ_n, $n = 1, 2$, are the investment adjustment cost parameters, κ is the capital reallocation cost parameter,[8] and W_1 and W_2 are two independent Brownian motions. The parameter ρ_{12} denotes the instantaneous diffusive correlation coefficient between the Brownian shocks of the two capital stocks. N_e and N_c are two independent point process capturing disaster risk. Since

[6] We could have adopted a more realistic production structure with imperfect substitution between the two final goods, i.e., $Y = F(Y_1, Y_2)$, where F is for instance the CES aggregator. Also, each sector could have both types of energy and capital stocks as production factor. Further, one could argue that once the energy transition from coal to solar energy has taken place, electricity is a uniform good (see Hassler et al. 2020). However, we have chosen this stylized structure to focus on our key idea.

[7] For notational convenience, we drop the time index t when it does not create confusion. Furthermore, K_{n-} is short for K_{nt-}, i.e., for the left-limit of K_n at time t. Notice that for the $\mathrm{d}t$ and $\mathrm{d}W$ terms this distinction is irrelevant since the point process N only jumps at countably many time points and Lebesgue and Brownian integrands can be changed at countably many points.

[8] We assume that the green sector incurs the capital reallocation costs.

these disaster shocks are common for both types of capital, they significantly increase the total correlation between the two capital stocks.[9]

The process N_e models macroeconomic disasters whose jump intensity λ_e is constant as in Barro (2006, 2009) and Barro and Jin (2011). The process N_c models climate disasters as in Karydas and Xepapadeas (2019). This is the *second channel* by which climate change can affect the economy. Its jump intensity $\lambda_c = \lambda_c(T)$ depends on current temperature T. Here, $\lambda_i \mathrm{d}t$ is the probability for a jump to occur over the small time interval $\mathrm{d}t$ and $1/\lambda_i$ is the expected waiting time to the next jump, $i \in \{e, c\}$. The parameters ℓ_e and ℓ_c are the corresponding jump sizes which are stochastic, but independent of the Brownian and Poisson shocks in the model. For simplicity, we suppose that the jump sizes are the same for both types of capital.

Our model has two channels by which climate damages affect the economy: via the damage functions $D_i(T)$ scaling down output in response to climate change as in the DICE model; the disaster probability might increase in temperature as in Bansal et al. (2019) and Karydas and Xepapadeas (2019).

2.3 Emissions and Temperature

Following Allen et al. (2009), Matthews et al. (2009), and IPCC (2014), we assume that—up to some environmental stochastic shocks—global average temperature T is driven by cumulative emissions $E_t = \int_0^t \varepsilon_s \mathrm{d}s$ measured in gigatons of carbon (GtCs). Global average temperature (above the pre-industrial level) is thus given by

$$T_t = T_0 + \vartheta E_t + \int_0^t \sigma_T \mathrm{d}W_{3s},$$

where T_0 is current temperature and ϑ denotes the transient climate response to cumulative emissions (TCRE). W_3 denotes a third standard Wiener process that is independent of W_1 and W_2. The diffusion coefficient σ_T is constant. Current emissions are $\varepsilon = \nu F_2$ where F_2 is the rate of fossil use in energy units and $\nu = \nu(t, T, K_1, K_2)$ the emission intensity per unit of fossil fuel,

[9] Total correlation thus involves both the instantaneous correlation stemming from Brownian shocks and common jump risk, see Section 4.1.

which depends on technological progress and thus might be state dependent. Consequently, we have

$$\mathrm{d}T = \beta F_2 \mathrm{d}t + \sigma_T \mathrm{d}W_3, \tag{2.4}$$

where $\beta = \vartheta\nu$ and thus β might depend on t, T, K_1, and K_2. We calibrate the emission intensity such that business-as-usual (BAU) emissions are close to the uncontrolled path in the latest version of DICE, see Nordhaus (2017).[10] Additionally, $\varepsilon = 0$ if $K_2 = 0$, i.e., there are no carbon emissions if the dirty capital stock has been fully phased out.

2.4 Dividends, Consumption, and Preferences

The dividend is defined as the residual cash flow net of investments and energy costs,[11] $D_n = Y_n - I_n - b_n F_n$, where b_1 denotes the cost of one unit of renewable energy and b_2 the cost of one unit of fossil fuel.[12] For simplicity, we make the bold assumption that the costs of one unit of fossil fuel or renewable energy are exogenous and not affected by exogenous rates of technical progress (e.g., ongoing hikes in green innovation or the shale gas revolution). In equilibrium, aggregated dividends equal aggregate consumption, i.e., $C = D_1 + D_2$. Our economy has identical agents with recursive preferences. As shown in Duffie and Epstein (1992b),[13] these preferences are the continuous-time version of discrete-time recursive utility developed in Kreps and Porteus (1978) and Epstein and Zin (1989). As in Wachter (2013), we assume unit elasticity of intertemporal substitution (EIS = 1). The coefficient γ of relative risk aversion (RRA) can be chosen independently and typically exceeds unit EIS to reflect a preference for early resolution of uncertainty.

The value function (or indirect utility function) J is thus recursively defined by

$$J(t, K_1, K_2, T) = \sup_{I_1, I_2, R, F_1, F_2} \mathbb{E}_t\Big[\int_t^\infty f(C_s, J(s, K_{1s}, K_{2s}, T_s)\mathrm{d}s\Big], \tag{2.5}$$

[10] The BAU scenario for the decentralized market economy occurs when policy makers do not impose carbon taxes.

[11] Following van den Bremer and van der Ploeg (2019), we have constant energy costs. It is however possible to model technological process via time-varying energy costs as in Golosov et al. (2014). These results do not vary significantly and are available upon request.

[12] Some authors define dividends as levered consumption $D_n = C_n^\varphi$ for a leverage parameter $\varphi > 1$ to model a higher volatility of dividends compared to consumption (e.g., Bansal and Yaron 2004; Benzoni et al. 2011; Wachter 2013; Branger et al. 2016).

[13] They refer to this class of preferences as stochastic differential utility (SDU).

where f is the aggregator determining preferences. For unit EIS and an arbitrary level of risk aversion γ, this aggregator takes the form

$$f(C,J) = \begin{cases} \delta(1-\gamma)J\log\Big(\frac{C}{[(1-\gamma)J]^{\frac{1}{1-\gamma}}}\Big), & \gamma \neq 1, \\ \delta\big[\log(C) - J\big], & \gamma = 1, \end{cases}$$

where C denotes consumption and δ the rate of time impatience. Notice that f depends on the value function J, which reflects the recursive structure of the preferences. For $\gamma = 1$, the preference structure collapses to time-additive logarithmic utility.

3 Optimality and the Social Cost of Carbon

The value function $J = J(t, K_1, K_2, T)$ satisfies the Hamilton-Jacobi-Bellman (HJB) equation. Following Duffie and Epstein (1992b), this equation is

$$\begin{aligned} 0 = \max_{I_1,I_2,R,F_1,F_2} \Bigg\{ & J_t + \delta(1-\gamma)J\log\Big(\frac{Y_1+Y_2-I_1-I_2-b_1F_1-b_2F_2}{[(1-\gamma)J]^{\frac{1}{1-\gamma}}}\Big) + J_T\beta F_2 \\ & + \frac{1}{2}J_{TT}\sigma_T^2 + J_{K_1}\Big(I_1 - \frac{1}{2}\phi_1\frac{I_1^2}{K_1} + R - \frac{1}{2}\kappa\frac{R^2}{K_1} - \delta_1^k K_1\Big) + \frac{1}{2}J_{K_1K_1}K_1^2\sigma_1^2 \\ & + J_{K_2}\Big(I_2 - \frac{1}{2}\phi_2\frac{I_2^2}{K_2} - R - \delta_2^k K_2\Big) + \frac{1}{2}J_{K_2K_2}K_2^2\sigma_2^2 + J_{K_1K_2}K_1K_2\sigma_1\sigma_2\rho_{12} \\ & + \lambda_e\mathbb{E}[J(K_1(1-\ell_e), K_2(1-\ell_e), T) - J] + \lambda_c(T)\mathbb{E}[J(K_1(1-\ell_c), K_2(1-\ell_c), T) - J]\Bigg\} \end{aligned} \tag{3.1}$$

where subscripts of J denote partial derivatives, e.g., $J_{K_1} = \frac{\partial J}{\partial K_1}$. The first-order optimally conditions give rise to efficiency conditions (3.2) – (3.5).

3.1 Optimal Policies

Optimal investment in sector $n \in \{1, 2\}$ reads

$$I_n = \frac{K_n}{\phi_n}\frac{q_n - 1}{q_n}, \tag{3.2}$$

where ϕ_n captures the strength of the intertemporal adjustment costs and

$$q_n = \frac{C}{\delta(1-\gamma)} \frac{J_{K_n}}{J}, \qquad n = 1, 2, \tag{3.3}$$

is Tobin's Q of sector n. Condition (3.2) for investment in sector n shows that investment rates are small if intertemporal adjustment costs are high and large if the sectoral Tobin's Q is high. The sectoral Tobin's Q is defined as the marginal value of capital converted into utility units. It equals the ratio of market value to the replacement cost of physical value. The sectoral Tobin's Q is bigger than one, since installing capital is costly and installed capital earns a rent in equilibrium.

The optimal reallocation from dirty to green capital is

$$R = \frac{K_1}{\kappa} \frac{q_1 - q_2}{q_1}. \tag{3.4}$$

The rate at which carbon-intensive capital is converted into carbon-free capital is proportional to the carbon-free capital stock. Reallocation decreases in the Tobin's Q of the dirty sector and increases in the Tobin's Q of the green sector. This conversion rate is small if intratemporal adjustment costs are high.

The optimal use of green energy and fossil fuel follow from

$$\eta_1 A_1 \Big(\frac{F_1}{K_1}\Big)^{\eta_1 - 1} \Lambda_1(T) = b_1, \qquad \eta_2 A_2 \Big(\frac{F_2}{K_2}\Big)^{\eta_2 - 1} \Lambda_2(T) = b_2 + \tau_f, \tag{3.5}$$

where the optimal Pigouvian social cost for using one unit of fossil fuel is

$$\tau_f = \frac{\beta C}{\delta(\gamma - 1)} \frac{J_T}{J}. \tag{3.6}$$

The marginal product of the green capital stock is equal to the marginal cost of one unit of green energy. For the dirty capital stock, the marginal revenue equals the marginal costs plus the external effects of emitting carbon. The social cost of burning one ton of carbon or SCC for short is

$$\tau_c = \frac{\tau_f}{\nu} = \frac{\vartheta C}{\delta(\gamma - 1)} \frac{J_T}{J}, \tag{3.7}$$

where ν is the emission intensity per unit of fossil fuel defined in Section 2.3. The optimal SCC increases in consumption reflecting that higher economic activity leads to higher carbon taxes (e.g., Nordhaus 1991; Golosov et al. 2014; Rezai and van der Ploeg 2016).

The share of dirty capital to total capital is

$$S = \frac{K_2}{K_1 + K_2} \tag{3.8}$$

which indicates the carbon-intensity of the economy. We denote the total stock of capital by $K = K_1 + K_2$. During the transition to a low-carbon economy, carbon-free capital is gradually replacing dirty capital so that the share of dirty capital S decreases over time. Appendix A shows that the value function J can be reformulated in terms of temperature T and the new state variable S instead of T, K_1, and K_2 (see Proposition A.1). This reformulation significantly simplifies our numerical solution approach as described in Appendix C.1.

3.2 Decentralizing the Social Optimum in the Market Economy

One way to ensure that the social optimum is attained in the decentralized market economy is to price carbon (either via a global carbon tax or via a global cap-and-trade system) at a price equal to the optimal SCC and to subsidize capital in sector n at a rate equal to $(1 - \eta_n - \alpha_n)Y_n/K_n$. The net revenue of the carbon tax and the capital subsidies to the two sectors is refunded in lump-sum fashion to the private sector. If this is done, the first-order optimality conditions for the market economy coincide with those of the social optimum. The carbon tax is needed to internalize the global warming externality and the capital subsidies are needed to correct for the fact that firms do not internalize the beneficial effect of capital accumulation (including knowledge creation) on the productivity of labor in other firms.

4 Calibration

This section discusses the benchmark calibration of our model. Table 1 summarizes the calibration details. Further details can be found in Appendix D.

	Preferences	
δ	time-preference rate	0.05
γ	relative risk aversion	5.288
ψ	elasticity of intertemporal substitution	1
	Economic Model	
Y_0	initial GDP (trillion US \$)	75.8
S_0	initial share of dirty capital	0.94
A_1	green productivity	0.851
A_2	brown productivity	0.828
b_1	fossil fuel costs (\$ per tC)	540
b_2	green energy costs (\$ per etC)	810
η_n	energy share in production	0.066
ϕ_n	investment adjustment cost parameter	18.12
σ_n	annual capital volatility	0.02
α_e	macroeconomic jump size parameter	8
λ_e	macroeconomic disaster intensity parameter	0.088
κ	capital reallocation cost parameter	1
ρ_{12}	instantaneous correlation	0
	Climate Model	
T_0	initial temperature (°C)	1
σ_T	temperature diffusion coefficient	0.015
ϑ	TCRE (°C/TtC)	1.8
p_0	emission intensity parameter	11.03
p_1	emission intensity parameter	0.1979
p_2	emission intensity parameter	-8.554×10^{-4}

Table 1: Benchmark Calibration. This table summarizes the parameters of the benchmark calibration with 2015 as base year. It is described in Section 4.

4.1 Economic Growth

In the past, the influence of climate change on asset markets has been negligible and the historical impact of climate change on the economy has been, if anything, moderate, at least in developed countries (e.g., Dell et al. 2009, 2012). We first calibrate production by disregarding climate damages. We then calibrate the damage specification.

Capital Shocks We set annual volatility of capital diffusion risk to $\sigma_1 = \sigma_2 = 0.02$ matching the observed volatility of consumption or output (e.g., Wachter 2013). We start with a

benchmark value of $\rho_{12} = 0$ for the *instantaneous correlation* between the two capital stocks.[14] Section 5 discusses the influence of this correlation and presents the effects if ρ_{12} is varied. We emphasize that, apart from instantaneous correlation ρ_{12} the correlation between the two capital stocks and, in turn, between asset prices is driven by macroeconomic disasters. Since both capital stocks are exposed to macroeconomic shocks via N_e, the total correlation between the capital stocks is significantly higher than indicated by the value of ρ_{12}. In our numerical simulations total correlation is always higher than 90%.

We assume that the recovery rates, $Z_i = 1 - \ell_i$, $i \in \{e, c\}$, have power distributions over $(0, 1)$ with parameters $\alpha_i > 0$, i.e., the jump size distribution is determined by the density function $\zeta_i(Z_i) = \alpha_i Z_i^{\alpha_i - 1}$, $Z_i \in (0, 1)$ (see Pindyck and Wang 2013). This specification is analytically tractable and the n^{th} moment of the recovery rate is $\mathbb{E}[Z_i^n] = \frac{\alpha_i}{\alpha_i + n}$. To calibrate the macroeconomic jump-size distribution, we follow Barro and Jin (2011) and define a disaster as an event destroying more than $\overline{\ell}_e = 10\%$ of GDP or aggregate consumption. They use historical consumption data to estimate an annual disaster probability of 0.038 and an average consumption loss of 20% when a disaster occurs: $\mathbb{E}[\ell_e | \ell_e > \overline{\ell}_e] = 0.2$ and $\lambda_e \int_0^{1-\overline{\ell}_e} \zeta_e(Z_e) \mathrm{d}Z_e = 0.038$. These can be solved to give $\alpha_e = 8$ and $\lambda_e = 0.088$.

Production and Energy Costs Ignoring the effects of climate change, the optimal SCC is zero and optimal energy use implies a linear production function $Y_n = A_n^* K_n$, with productivity

$$A_n^* = A_n^{\frac{1}{1-\eta_n}} \left(\frac{\eta_n}{b_n} \right)^{\frac{\eta_n}{1-\eta_n}}. \tag{4.1}$$

To calibrate time preference, risk aversion, adjustment costs and total factor productivity, we use a special case of our model with an aggregate capital stock (see Appendix D). Following Pindyck and Wang (2013), we choose these parameters to match a real expected growth rate of consumption of 2%, an average consumption fraction of GDP of 75%, an initial risk-free interest rate of $r_0^f = 0.8\%$ per annum, an average equity premium of 6.3% per annum, and a Tobin'Q of 1.5. We use this to back out a time-preference rate of $\delta = 0.05$ per annum, a degree of relative risk aversion of $\gamma = 5.288$, adjustment cost parameters of $\phi_1 = \phi_2 = 18.12$, and total factor productivities of $A_1^* = A_2^* = 0.1$.[15]

[14] This is also assumed by Cochrane et al. (2007) for an endowment economy.

[15] We do this by solving the non-linear system of equations (D.1)-(D.5).

Specification	Calibration
Level Impact (L–I)	$\theta_i = 0.00236$
Disaster Impact (D–I)	$\lambda_c(T) = 0.003 + 0.096T$, $\alpha_c = 65.67$

Table 2: Two Types of Specifications for Global Warming Damages. The table summarizes the different damage specifications that are studied in this paper.

Following van den Bremer and van der Ploeg (2019), we use energy shares $\eta_i = 0.066$ and set the cost of fossil fuel to $b_2 = \$540/\text{tC}$. We use a significantly higher price of green energy, i.e., $b_1 = \$810/\text{etC}$, which is in line with production costs in developed countries such as Germany. Solving (4.1) for A_i yields the sector-specific productivities $A_1 = 0.851$ and $A_2 = 0.828$. Finally, we choose the reallocation cost parameter $\kappa = 1$ such that the model-predicted optimal global average temperature increase is approximately 4°C after 200 years, which is in line with the optimal temperature evolution in the latest version of DICE (see Nordhaus 2017).

4.2 Damage Specifications

Table 2 specifies our two different damage specifications.

Level Impact (L–I) The standard damage function in DICE is inverse quadratic. Nordhaus (2017) uses the parametrization $\Lambda(T) = \frac{1}{1+\theta_i T^2}$ and calibrates the damage function so that damages at 3°C are 2.08% of pre-damages output. This gives $\theta_i = 0.00236$.

Disaster Impact (D–I) Karydas and Xepapadeas (2019) collect data on climate-related events for 42 countries over the period from 1911 to 2015.[16] Following the methodology of Loayza et al. (2012), they estimate climate-related disaster probabilities and magnitudes. Their model involves time-varying temperature disaster risk where the disaster intensity follows a mean-reversion process whose long-term mean is linear in temperature, $\overline{\lambda}_c(T) = \overline{\lambda}_{c0} + \overline{\lambda}_{c1}T$. Abstracting from mean reversion, we set $\lambda_c(T) = \lambda_{c0} + \lambda_{c1}T$ with $\lambda_{c0} = 0.003$ and $\lambda_{c1} = 0.096$. The process $\lambda_c(T)$ is approximately the probability that a disaster hits within the period of a year. Karydas and Xepapadeas (2019) also report a mean magnitude of $\mathbb{E}[\ell_c] = 1.5\%$ of climate-related disasters. Using a power distribution for the recovery rate Z_c yields $\alpha_c = 65.67$.

[16] They use a database called the international disasters database EM-DAT, which is available at https://www.emdat.be/

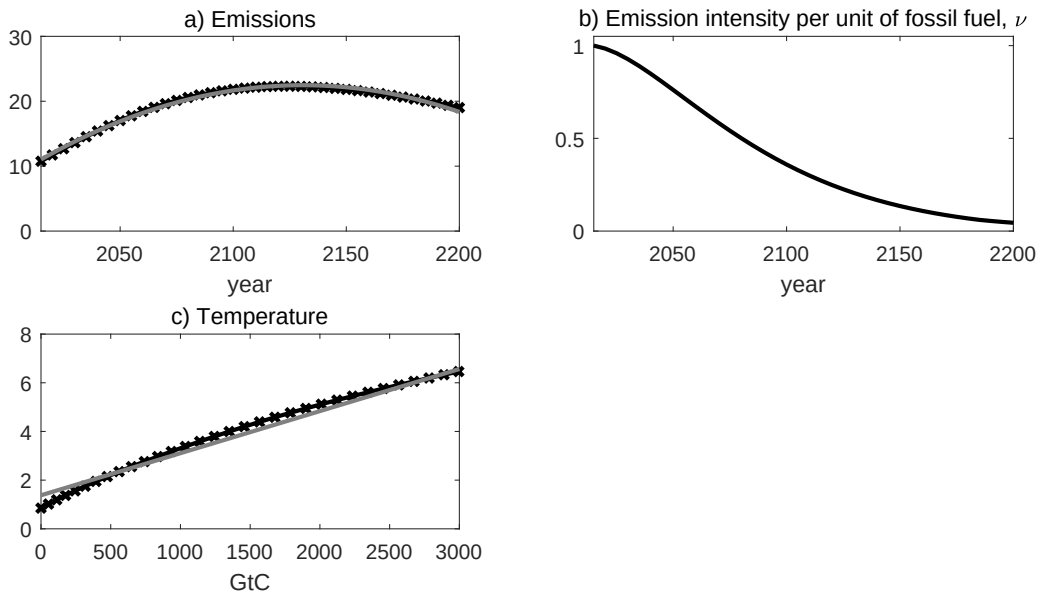

Figure 1: Calibration of the Climate System. Panel (a) shows carbon dioxide emissions in the BAU scenario in DICE (black crosses). The gray line depicts the BAU evolution in our model. The emission intensity per unit of fossil fuel is plotted in Panel (b). Panel (c) shows the relation of cumulative emissions and temperature increase in DICE. The gray line shows a linear least-squares fit to this data. The slope of this straight line gives a Transient Climate Response to Cumulative Emissions (TCRE) of 1.8°C/TtC.

4.3 Climate Model

Carbon Emissions We calibrate the emission intensity per unit of fossil fuel ν such that in the business-as-usual (BAU) scenario, the model matches the BAU carbon emissions in DICE-2016R. We set $\nu(t, K_1, K_2) = \frac{p(t)}{K_1+K_2}$, where $p(t) = p_0 + p_1 t + p_2 t^2$. A least-squares fit yields $p_0 = 11.03$, $p_1 = 0.1979$, and $p_2 = -8.554 \times 10^{-4}$. Carbon emissions are thus $\varepsilon_t = p(t) S_t f_{2t}$. This calibration ensures that carbon emissions are zero if the dirty capital stock is not used and production of dirty goods is zero. The emission intensity tends to decrease over time as in DICE-2016R. Panel (a) of Figure 1 depicts the calibration of the carbon emissions and shows that the model is well in line with the latest version of DICE (Nordhaus 2017). Panel (b) depicts the expected path of the normalized emission intensity per unit of fossil fuel use, $\mathbb{E}[\nu_t]/\nu_0$, under BAU.

TCRE Recent studies estimate a transient climate response to cumulative carbon emissions of 0.8 to 2.4°C/TtC (e.g., Allen et al. 2009; Matthews et al. 2009, 2018). We take a TCRE of $\beta = 1.8$°C/TtC, which is in line with DICE, see Panel (c) of Figure 1.

5 Optimal Climate Policies

5.1 Abatement and Diversification Motives

To understand the economic channels driving our results, notice that there are two opposing effects: First, dirty capital causes a negative externality that diminishes output. Therefore, the agent seeks to reduce the share of dirty capital to reduce carbon dioxide emissions. This is the *abatement motive*. Second, the agent is risk averse and thus dislikes volatility. Therefore, the economy also seeks to reduce total capital volatility which is driven by the share of dirty capital. This is the *diversification motive*.

For high *and* low values of the share of dirty capital the economy is poorly diversified. Initially dirty capital dominates the capital stock and thus the economy is not well-diversified. Therefore, the diversification motive accelerates climate action until full diversification is reached. At this level, abatement and diversification become conflicting targets and the transition towards a low-carbon economy is slowed down from this point onwards. Nevertheless, the economy does not stop at the level of full diversification. Instead, the overall optimum, which takes climate objectives into account, is below the level of full diversification.

The question arises whether the abatement motive or the diversification motive dominates and by how much the abatement motive shifts the optimal level below the level of full diversification. The answer to this question critically depends on the strength of the damage specification and the instantaneous correlation between the two capital stocks. Especially for low correlation and moderate damages, the abatement motive is significantly dampened by the diversification motive. On the other hand, even in a hypothetical model without damages from climate change, the diversification motive incentivizes the economy to reallocate from the green to the dirty capital stock until full diversification is reached. In the remainder of this section, we will explore the strength of these different motives.

In our benchmark setup, both sectors are identically calibrated if climate change is disregarded. In this case, the economy reaches full diversification if both capital stocks are of the same size.

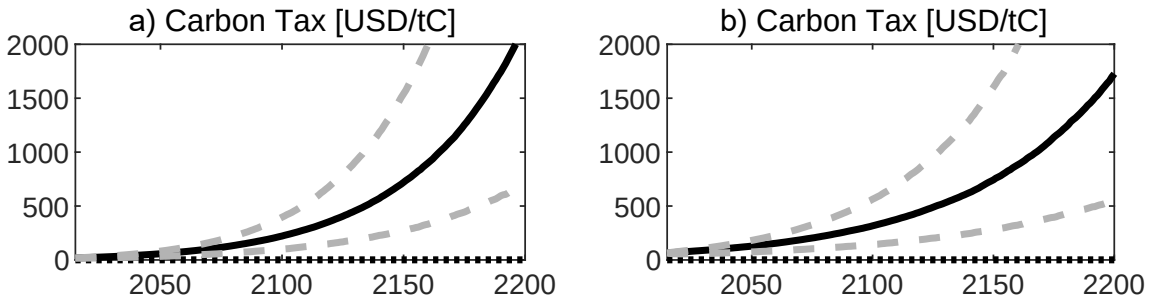

Figure 2: Optimal Carbon Taxes. The figure depicts the simulation of the optimal carbon prices for the two damage specifications level impact (1st column) and disaster impact (2nd column) until the year 2200. Median optimal paths are depicted by solid lines (——) and median BAU paths by dotted lines (·····). Dashed lines (- - -) show 5% and 95% quantiles of the optimal solution.

This also happens to be the share that minimizes the variance of the total capital stock. With climate change it is optimal to reduce the share of dirty capital below 50%. Any deviation from 50% is thus a consequence of the global warming externality. We show below that qualitatively our results carry over to settings with heterogeneous sectors. However, it turns out that the effect of climate change on diversification is most significant if the dirty sector has a low capital volatility compared to the green sector.

Notice that in this section we report shares of capital. From an asset-pricing perspective, one might wonder what the results look like if we calculate the values of each sector and report shares based on these valuations. This question can only be addressed in an equilibrium asset-pricing framework as presented in Section 6. However, in robustness checks based on values we have verified that the corresponding shares are almost identical to the ones based on capital. Therefore, we only present the results based capital shares.[17]

5.2 Policy Simulation Results

We assume that the initial share of dirty capital is 94% to reflect that due to the various types of investment adjustment and relocation costs the world economy is currently in an undiversified state even when climate policy is not implemented. Initially, there is thus too much of the dirty and too little of the green capital stock. Recall that the fully diversified share is 50% for our calibration if the externality coming from climate damage is disregarded. With this externality, the share is lower. We also refer to Appendix F, which provides further simulation results for

[17]The results based on shares of value are available upon request.

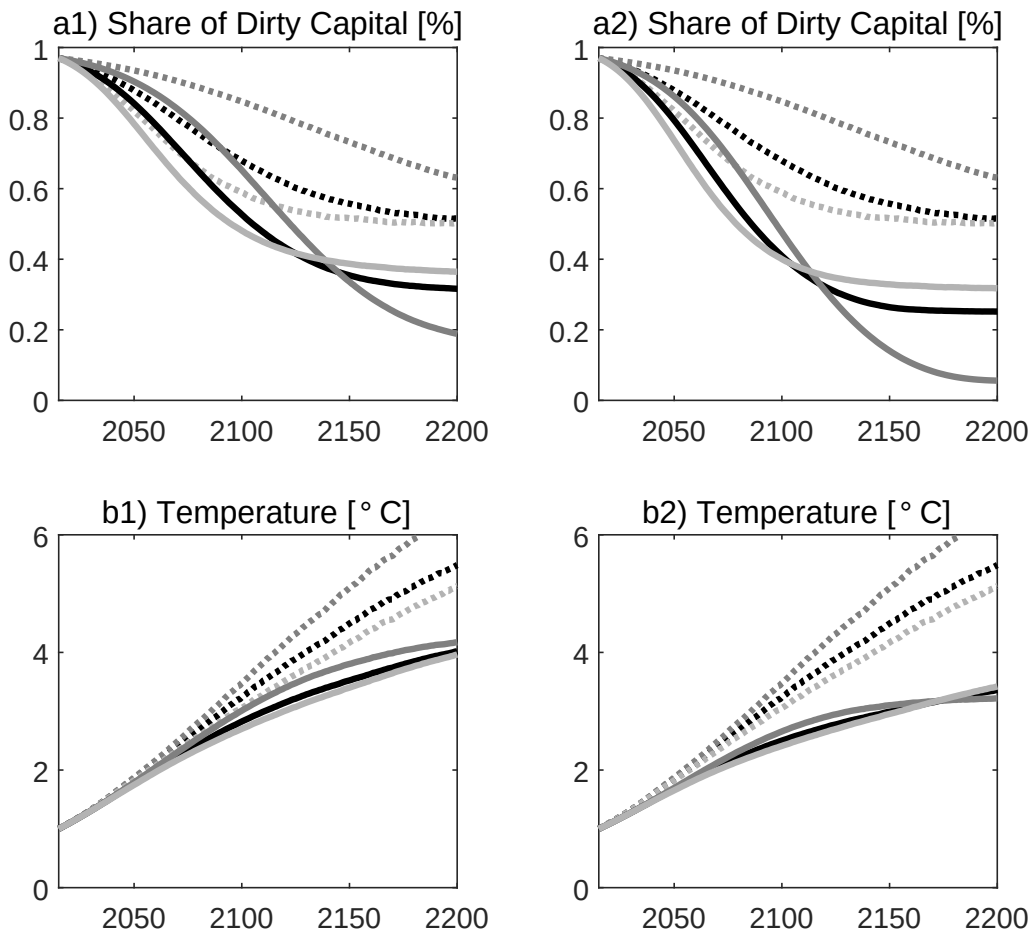

Figure 3: Varying the Correlation Coefficient. Solid lines depict the optimal evolution of the share of dirty capital and global average temperature for the two damage specifications level impact (1st column) and disaster impact (2nd column) until the year 2200. Black lines (⋯⋯, ——) show results for the benchmark case where the correlation between the Brownian shocks affecting the green and dirty sector is $\rho_{12} = 0$. Gray lines (⋯⋯, ——) show results with $\rho_{12} = 0.5$. Light lines (⋯⋯, ——) depict the results with $\rho_{12} = -0.5$. Dotted lines show the corresponding results for hypothetical scenarios without damages from climate change. The main insight from this figure is that initially it is important to drive down the carbon-intensive part of the economy for both diversification and abatement reasons, but once the share of dirty capital has fallen below its optimal share in the absence of climate damages the carbon-intensive part of the economy is driven down purely for abatement reasons at the expense of the diversification objective.

economic and financial key variables. Before we delve into the time paths of the share of dirty capital, temperature, Figure 2 shows the median optimal carbon price and their 5% and 95% quintiles for the benchmark case. In line with the literature, carbon prices roughly rise in line with GDP.

Effects of Correlation between the Two Sectors The correlation between asset returns plays a crucial role for the optimal asset allocation and, in turn, for asset pricing. This section thus explores the role of the correlation coefficient ρ_{12} between the diffusive shocks to the capital stocks. Figure 3 depicts the optimal evolution of the share of dirty capital for various combinations of the correlation coefficient and for the two damage specifications level impact (1^{st} column) and disaster impact (2^{nd} column) until the year 2200. Black lines (⋯⋯,——) show results for the benchmark case $\rho_{12} = 0$. Gray lines (⋯⋯, ——) show results for $\rho_{12} = 0.5$. Light lines (⋯⋯, ——) depict results for $\rho_{12} = -0.5$. The correlation between the two capital stocks and, in turn, between asset prices is significantly driven by macroeconomic disasters. Since both capital stocks suffer common macroeconomic shocks via N^e, the true correlation between the capital stocks is significantly higher than ρ indicates. Our numerical simulations show that the true correlation is always higher than 90%. Dotted lines depict results for hypothetical scenarios without damages from climate change.[18] In these scenarios, there is no benefit from climate action. Therefore, only the diversification motive matters and the agent reallocates capital from the green to the dirty stock until full diversification, $S = 50\%$, is reached.

If climate damages are internalized by policy makers, the abatement motive matters. In turn, the share of dirty capital stabilizes at a social optimum below full diversification, $S = 50\%$. With zero correlation (⋯⋯,——), the optimal share of dirty capital stabilizes between 20% and 30% depending on the damage specification. It does not go to zero, as some dirty capital is kept for diversification purposes. The differences between the dotted and solid lines thus result from the benefits of combating global warming.

A negative correlation coefficient (⋯⋯, ——) amplifies the diversification motive. This leads to a faster transition to full diversification of $S = 50\%$. In the short run, this effect accelerates decarbonization of the economy, but in the long run the opposite is true, see Panels a1)-a3) of Figure 3. The economy keeps a higher share of dirty capital to benefit from diversification. In turn, the transition is slowed down and ends at a higher steady-state share of dirty capital compared to the case with zero correlation. In other words, there is less climate action in the long run if the benefits from diversification are more pronounced.

For a positive correlation coefficient, the diversification motive is less important, which can be seen from the gray dotted lines (⋯⋯). In the short run, transition from a carbon-intensive to a carbon-free economy is significantly slowed down. In the long run, however, the abatement

[18] This is different from the BAU scenario where there are damages from climate change, but they are not corrected for by the policy makers.

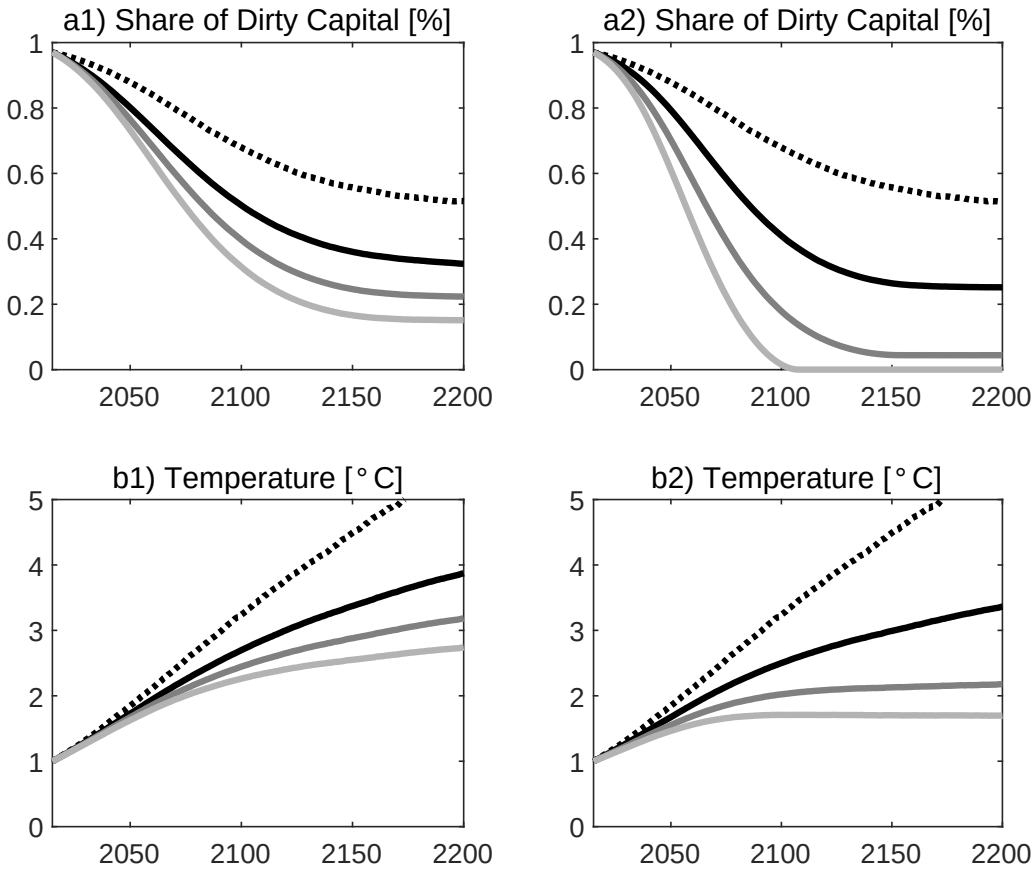

Figure 4: Increasing Intensities of Global Warming Damages. The figure depicts the simulation of the share of dirty capital and global average temperature for the two damage specifications level impact (1st column) and disaster impact (2nd column) until the year 2200. The black dotted lines (·····) show the results for a hypothetical scenario without damages from climate change. The black solid lines (——) show the results for the damage parameters as calibrated in Section 4. The gray lines (——) show results with damage parameters that are twice as high as in the benchmark calibration. The light lines (——) show results with damage parameters that are three times higher than those from the benchmark calibration. The main insight from this figure is that with higher intensities of damages than our benchmark damages, the abatement motives becomes relatively more important than the diversification motive and leads to a lower or even a zero dirty capital stock in the long run.

motive dominates and the share of dirty assets stabilizes at lower levels (——). Hence, the speed of decarbonization is significantly effected by the sign and size of the correlation coefficient between the green and dirty capital stock.

Effects of Different Damage Specifications Figure 4 depicts the influence of the damage specification on the optimal evolution of the share of dirty capital and global temperature.

Impact	Benchmark (——)	Double Impact (——)	Triple Impact (——)
Level	$\theta_i = 0.00236$	$\theta_i = 0.00472$	$\theta_i = 0.00708$
Disaster	$\lambda_c(T) = 0.003 + 0.096T$	$\lambda_c(T) = 0.003 + 0.192T$	$\lambda_c(T) = 0.003 + 0.288T$

Table 3: Different Intensities for the Specifications of Global Warming Damages. The table summarizes the different damage specifications that are used in Figure 4.

The black dotted lines (·····) show the results for a hypothetical scenario where climate change does not generate economic damages, in which case only the diversification motive matters. If economic damages from climate change are pronounced, the abatement motive comes into play and the optimal level of the share of dirty capital shifts down to a social optimum below $S = 50\%$. The black solid lines (——) show the results for the damage parameters presented in Section 4. The gray lines (——) depict results with damage parameters that are twice as high. The light lines (——) show results with damage parameters that are three times higher. Table 3 summarizes the damage parameters that are used in Figure 4. It can be seen that for higher damage parameters the abatement motive becomes more pronounced and the diversification motive loses its importance. For sufficiently high damages, the dirty capital stock vanishes and production of carbon-intensive goods ceases. This increases the volatility of total capital, but the benefits from abatement eventually dominate the benefits from diversification. Doubling or tripling the damage parameter for the disaster impact has a huge influence. The effect for the level impact is less pronounced.

Effect of Heterogeneous Volatilities So far, we have considered specifications where the calibration of the sectors is identical in the absence of climate change. Now, we analyze situations with heterogeneous capital volatilities. We fix the capital volatility of the green sector at $\sigma_1 = 0.02$ and vary the volatility of the dirty sector, $\sigma_2 \in \{0.02/\sqrt{2}, 0.02, 0.02\sqrt{2}\}$ (corresponding to "low risk", benchmark, "high risk"). Figure 5 depicts the corresponding results. If we disregard the effect of climate change, then the optimal long-term shares of the dirty sector are 2/3, 1/2, and 1/3 (dotted lines). An interesting effect arises if we take climate change into account. As can be seen from the results for the Nordhaus calibration in Panel a1), the relative reduction of the dirty sector resulting from climate damages is most significant if the volatility of the dirty sector is small, i.e., if the dirty sector has a high diversification potential ("low risk") without damages from climate change (····· vs. ——). In this case, the optimal share of the dirty sector drops from 66% to 36%. In the benchmark case, this share is 32% instead of 50%. In the

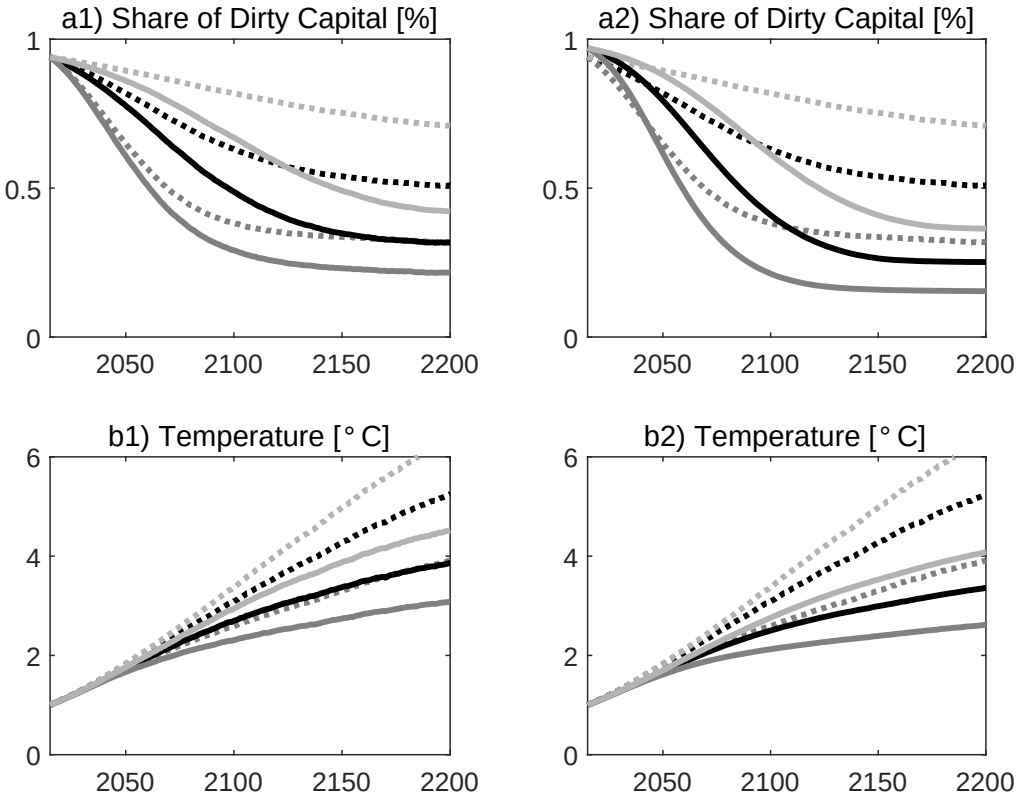

Figure 5: Heterogeneous Volatilities. Solid lines depict the optimal evolution of the share of dirty capital and global average temperature for the two damage specifications level impact (1^{st} column) and disaster impact (2^{nd} column) until the year 2200. Dotted lines show the results for hypothetical scenarios without damages from climate change. Black lines (⋯⋯,——) show results for the benchmark case where the volatilities are identical. Gray lines (⋯⋯, ——) show results for a higher volatility of shocks to the dirty sector, $\sigma_2 = 0.02\sqrt{2} = 0.0282$. Light lines (⋯⋯, ——) depict the results for a lower volatility of shocks to the dirty sector, $\sigma_2 = 0.02/\sqrt{2} = 0.0141$. The main insight from this figure is that the impact of climate change on diversification is most significant if the dirty sector has a low capital volatility σ_2, in which case the share of dirty capital and temperature are higher than in the benchmark case. Effectively, the low volatility of the dirty capital sector prevents more ambitious climate action as dirty capital fulfills a useful diversification role.

high-risk scenario, the optimal share of the dirty sector drops from 33% to 22%. The reason for the more pronounced climate action in the low-risk environment becomes clear if we look at Panel b1) depicting the temperature paths. If there is no effect of climate change on capital (⋯⋯), then the temperature peaks at the highest level in the low-risk scenario. Therefore, the agent reacts the most if the damages are internalized (——). This is facilitated by the high level of dirty capital without climate change, i.e., there is room to lower the share of dirty capital. Consequently, the total effect of the abatement motive is the biggest in the low-risk scenario

even though the share of dirty capital and temperature are higher than in the benchmark case (·····,——). Our findings are confirmed by Panel a2) that shows the reductions for an jump impact from climate change.

6 Equilibrium Asset Prices

In this section, we price both the green and dirty assets in the economy. We first derive the stochastic discount factor of our economy and then provide equilibrium representations of the risk premia as well as of the risk-free rate.

6.1 Dynamics of the Stochastic Discount Factor

The information about the current value of future (uncertain) cash flows is summarized in the stochastic discount factor or SDF (also known as state-price deflator or pricing kernel). If the SDF is known, we can calculate today's price of any given cash-flow stream. It thus generalizes standard discount factor ideas (e.g., Cochrane 2005, pp. 6ff).

Duffie and Epstein (1992a) and Duffie and Skiadas (1994) show that for continuous-time recursive utility the SDF has the form

$$H_s = \exp\left(\int_0^s f_J(C_u, J_u)\, du\right) f_C(C_s, J_s), \tag{6.1}$$

where J_s denotes the time-s value of the value function. Applying Ito's lemma to (6.1) gives[19]

$$\frac{\mathrm{d}H}{H_-} = \frac{\mathrm{d}f_c(C_-, J_-)}{f_c(C_-, J_-)} + f_J(C, J)\mathrm{d}t, \tag{6.2}$$

where subscripts of f denote partial derivatives and J denotes the value function whose closed-form representation is given in Proposition A.1. Although the dynamics of the SDF have the compact representation (6.2), determining the explicit form involves several auxiliary calculations that can be found in Appendix B.1. The dynamics of the SDF contain several pieces of relevant information about key variables of the economy: its drift equals the equilibrium

[19] Again we drop time dependencies. The notation $_-$ is short for $t-$, i.e., the left limit at time t. We emphasize that for dt terms it does not matter whether we take left limits, since integrands of Lebesgue integrals can be changed on zero sets and the jumps of our point process constitute a zero set w.r.t. the Lebesgue measure.

risk-free interest rate (with a negative sign) and the coefficient in front of the Brownian shocks contains the market prices of diffusive risk, see Proposition 6.1 below.

Proposition 6.1 (Equilibrium)**.** *Let σ_k be the three-dimensional volatility vector of the total stock of capital, see (A.9), and σ_g be the three-dimensional volatility vector of G, see (B.1). Let μ_c and σ_c denote the drift rate and the three-dimensional volatility vector of optimal consumption, respectively, see (B.3) and (B.4). The SDF follows the dynamics*

$$\frac{\mathrm{d}H}{H_-} = -r^f \mathrm{d}t + \Theta_W^\top \mathrm{d}W + \sum_{i\in\{e,c\}} \big((1-\ell_i)^{-\gamma} - 1\big)\mathrm{d}N_i - \Theta_N \mathrm{d}t$$

with $W = (W_1, W_2, W_3)^\top$. The equilibrium risk-free rate r^f is

$$\begin{aligned} r_t^f = {} & \underbrace{\delta + \mu_c(t,S_t,T_t) - \gamma\|\sigma_c(t,S_t,T_t)\|^2}_{\textit{standard diffusion risk}} - \underbrace{\sum_{i\in\{e,c\}} \lambda_i(T_t)\mathbb{E}_t[\ell_i(1-\ell_i)^{-\gamma}]}_{\textit{disaster risk}} \\ & - \underbrace{\langle \sigma_g(t,S_t,T_t) + (\gamma-1)\sigma_c(t,S_t,T_t), \sigma_k(S_t) - \sigma_c(t,S_t,T_t)\rangle}_{\textit{temperature diffusion risk}} \end{aligned} \tag{6.3}$$

where $\|\cdot\|$ denotes the Euclidean norm and $\langle\cdot,\cdot\rangle$ the scalar product. The market price of diffusion risk and the market price of jump risk are

$$\begin{aligned} \Theta_{Wt} = {} & \underbrace{-\gamma\sigma_k(S_t)}_{\textit{standard risk}} + \underbrace{\sigma_g(t,S_t,T_t) + \sigma_k(S_t) - \sigma_c(t,S_t,T_t)}_{\textit{temperature risk}}, \\ \Theta_{Nt} = {} & \sum_{i\in\{e,c\}} \lambda_i(T_t)\mathbb{E}[(1-\ell_i)^{-\gamma} - 1]. \end{aligned}$$

Proposition 6.1 constitutes a similar decomposition of the risk-free interest rate as in Barro (2006, 2009), Pindyck and Wang (2013), and Wachter (2013). The first two terms in equation (6.3) also arise in deterministic models: if the time preference rate δ is high, there are strong preferences for early consumption and one would thus like to borrow. Since, in equilibrium, the risk-free asset is in zero net supply, the risk-free rate must increase to counter this. Besides, the risk-free rate increases in the expected growth rate of consumption $\mu_c(t,S_t,T_t)$ since it is desirable to smooth consumption. Notice that the EIS is one and thus the growth rate is multiplied by one.

The third term involves $\gamma\|\sigma_c(t, S_t, T_t)\|^2$ in equation (6.3). This represents the motive for precautionary savings in response to diffusion risk. In turn, the interest rate has to go down to keep the risk-free asset in zero net supply. The expected consumption growth rate and its volatility depend non-linearly on both the temperature and the dirty capital share, whereby the result is more involved and qualitatively different from one-tree endowment economies.

The fourth term $\sum_i \lambda_i(T_t)\mathbb{E}_t[\ell_i(1-\ell_i)^{-\gamma}]$ in equation (6.3) reflects precautionary savings in response to disaster risk. As for standard diffusion risk, these terms reduce the interest rate to keep the risk-free asset is in zero net supply. The greater the risk aversion, the greater is this effect, see also the extensive discussion in Wachter (2013). Notice that a novel feature is that the jump intensity for climate disaster risk λ_c increases in temperature and thus higher temperatures reduce the risk-free interest rate.

The last term $\langle \sigma_g(t, S_t, T_t) + (\gamma - 1)\sigma_c(t, S_t, T_t), \sigma_k(S_t) - \sigma_c(t, S_t, T_t)\rangle$ in equation (6.3) captures the interdependence between capital, consumption, and the value function. Compared to Cochrane et al. (2007) this term is new and results from the inability to hedge temperature shocks, i.e., it represents precautionary savings for uninsurable temperature risk. We emphasize that these components depend on the relevant state variables in a highly nonlinear manner. We calculate these variables numerically using finite differences, see Appendix C.2. An extensive discussion of theses effects in our calibrated model is given in Section 6.3.

6.2 Pricing Dividend Claims

We use the representation of the pricing kernel to calculate the ex-dividend price P_n of both assets in the economy. For the dividend stream D_n, the time-t price of asset n equals

$$P_{nt} = \mathbb{E}_t\Big[\int_t^\infty \frac{H_s}{H_t} D_{ns}\mathrm{d}s\Big]. \tag{6.4}$$

We denote the price-dividend ratio of asset n by $\Omega_n = P_n/D_n$. Its equilibrium expected excess return can be interpreted as the risk premium of the asset. It is formally given by the sum of its expected ex-dividend stock return, μ_{P_n}, plus its dividend yield, Ω_n^{-1}, minus the risk-free interest rate, r^f, so that

$$\mathrm{rp}_{nt} = \mu_{P_n t} + \Omega_{nt}^{-1} - r_t^f. \tag{6.5}$$

	r_f	μ_c	$-\gamma\|\sigma_c\|^2$	$-\langle\sigma_g + (\gamma-1)\sigma_c, \sigma_k - \sigma_c\rangle$
$T = 1°\text{C}$	0.82%	2.92%	–0.11%	0.00%
$T = 2°\text{C}$	0.77%	2.87%	–0.11%	0.00%
$T = 3°\text{C}$	0.71%	2.81%	–0.11%	–0.00%
$T = 4°\text{C}$	0.64%	2.74%	–0.11%	–0.01%
$T = 5°\text{C}$	0.55%	2.67%	–0.11%	–0.02%
$S = 0.05$	0.75%	2.94%	–0.19%	–0.00%
$S = 0.25$	0.76%	2.89%	–0.13%	–0.00%
$S = 0.50$	0.73%	2.83%	–0.11%	–0.00%
$S = 0.75$	0.66%	2.78%	–0.13%	0.00%
$S = 0.95$	0.53%	2.71%	–0.19%	–0.00%

Table 4: Risk-free Rate Decomposition for the Year 2100. The table shows the state-dependent terms in the decomposition of the risk-free rate (6.3). It provides sensitivity analysis for different values of temperature and the share of dirty capital around their median values in 2100 ($S = 0.53$, $T = 2.8$). The constant terms in (6.3) are the time preference rate $\delta = 0.05$, the contribution of economic disasters $\lambda_e \mathbb{E}_t[\ell_e(1-\ell_e)^{-\gamma}] = 0.0699$, and the contribution of climate-related disasters $\lambda_c \mathbb{E}_t[\ell_c(1-\ell_c)^{-\gamma}] = 0$.

The price-dividend ratio $\Omega_n = P_n/D_n$ satisfies the parabolic partial differential equation (B.9), which we solve numerically. The technical details are in Appendices B.3 and B.4.

6.3 Drivers of the Risk-Free Rates and of the Risk Premiums

Results for the Damage Calibration by Nordhaus Table 4 reports the decomposition of the risk-free rate into its state-dependent parts for the year 2100. The qualitative behavior is robust over time and similar for other years. In contrast to Karydas and Xepapadeas (2019), the drift rate of the consumption process μ_c and its volatility σ_c are endogenous. They depend on temperature and the share of dirty capital.

It can be seen that expected consumption growth μ_c decreases in both temperature and the share of dirty capital. The negative influence of temperature reflects the impact of climate change on output and is in line with other integrated assessment models. The negative influence of the share of dirty capital on consumption growth can be explained as follows. First, optimal fossil fuel decreases in the share of dirty capital. Since fossil fuel is a production factor, output is reduced and thus a high share of dirty capital negatively affects economic growth. Second, if the share of dirty capital is large, the agent reallocates capital at a higher rate which leads to higher capital adjustment costs and thus reduces consumption growth. Consequently, the risk-free rate decreases as well.

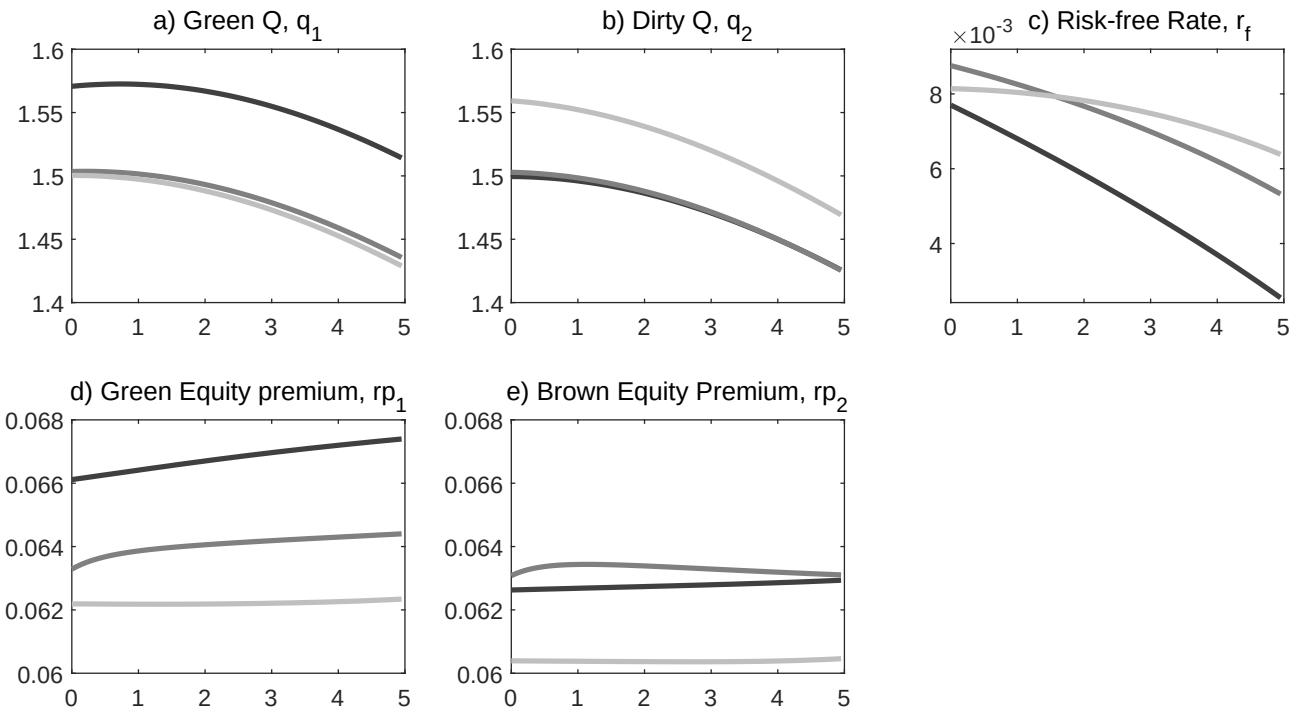

Figure 6: Asset Pricing versus Temperature and the Share of Dirty Capital (Nordhaus Damages). On the horizontal axis is temperature in the range from 0°C to 5°C. The lines represent various levels of the capital share: dark lines (——) depict $S = 0.95$, gray lines (——) refer to $S = 0.5$, and light (——) lines to $S = 0.05$. a) plots Tobin's Q of the green asset, b) shows Tobin's Q of the dirty capital stock, c) depicts the equilibrium risk-free rate, d) shows the risk premium of the green asset, e) depicts the risk premium of the dirty asset. The option to convert dirty capital into green capital generates interesting qualitative effects but the quantitative implications are modereate.

The consumption volatility is also state dependent. While the effect of temperature on the precautionary-savings term $\gamma\|\sigma_c\|^2$ is small, the share of dirty capital has a significant influence on the equilibrium risk-free rate. The latter result stems from a diversification argument as in Cochrane et al. (2007). Diversifying across the green and dirty capital stock reduces the volatility of the total capital stock and this effect carries over to aggregate consumption. This explains the non-monotonic behavior of the consumption volatility and, in turn, the non-monotonic relation between the share of dirty capital and the equilibrium risk-free rate.

Panels a) and b) of Figure 6 show that the Tobin's Q for both the green and the dirty sector decreases in temperature. The opposite is true for the book-to-market ratio. This implies that for a fixed amount of capital the market value decreases in temperature, both for the green and dirty asset. Panel a) shows that the Tobin's Q of the green asset increases in the share of dirty capital. Therefore, for a fixed amount of capital the green asset has a higher market

	Green Asset			Dirty Asset			Risk-free Rate
	rp_1	μ_{P_1}	Ω_1^{-1}	rp_2	μ_{P_2}	Ω_2^{-1}	r_f
$T = 1°\text{C}$	6.45%	2.82%	4.38%	6.30%	1.70%	5.35%	0.82%
$T = 2°\text{C}$	6.47%	2.94%	4.19%	6.28%	1.44%	5.50%	0.77%
$T = 3°\text{C}$	6.48%	3.02%	4.02%	6.26%	1.18%	5.64%	0.71%
$T = 4°\text{C}$	6.50%	3.08%	3.88%	6.25%	0.93%	5.78%	0.64%
$T = 5°\text{C}$	6.51%	3.10%	3.77%	6.24%	0.69%	5.90%	0.55%
$S = 0.05$	6.22%	1.99%	4.98%	6.03%	2.05%	4.73%	0.75%
$S = 0.25$	6.21%	2.02%	4.89%	6.09%	2.01%	4.77%	0.76%
$S = 0.50$	6.46%	2.89%	4.17%	6.29%	1.34%	5.55%	0.73%
$S = 0.75$	6.63%	4.11%	2.98%	6.21%	0.91%	5.76%	0.66%
$S = 0.95$	6.80%	5.82%	1.26%	6.30%	1.32%	5.25%	0.53%

Table 5: Risk Premium Decomposition for the Year 2100. The table shows the decomposition of the risk-premium rp_i into its components dividend yield Ω_i^{-1}, stock growth rate μ_{P_i}, and risk-free rate r_f. It provides sensitivity analysis for different values of the share of dirty capital and temperature around their median values in 2100 ($S = 0.53$, $T = 2.8$). We use the benchmark calibration from Section 4.

value if the economy is more carbon intensive. Panel b) indicates that the opposite is true for the carbon-emitting asset.

Panel c) shows the equilibrium risk-free rate whose behavior has been discussed above. Notice however that for low temperatures, the effect of the share of dirty capital on the risk-free rate is ambiguous which is due to the trade-off between the diversification and abatement motives.

Panels d) and e) depict the risk premia of the green and dirty asset, respectively. For the year 2100, Table 5 reports decompositions into the relevant components. Here μ_{P_n} denotes the expected ex-dividend stock return and Ω_n^{-1} the dividend yield of asset n. It turns out that the green risk premium rp_1 increases in both temperature and the share of dirty capital. The share of dirty capital has a significant positive influence on the risk premium while the effect of temperature is less pronounced. The same holds for the expected ex-dividend green stock return μ_{P_1} which sharply increases in the share of dirty capital. Notice that the opposite is true for its dividend yield Ω_n^{-1}. If the share of dirty capital is high, the green stock pays fewer dividends. When the transition to a low-carbon economy is completed, the green asset pays higher dividends. This is also in line with the positive relation between the share of dirty capital and the green Tobin's Q.

Panels d) and e) in Figure 6 show how the dirty and the green risk premium vary with temperature for given shares of dirty capital. Notice that the economy has the option to convert

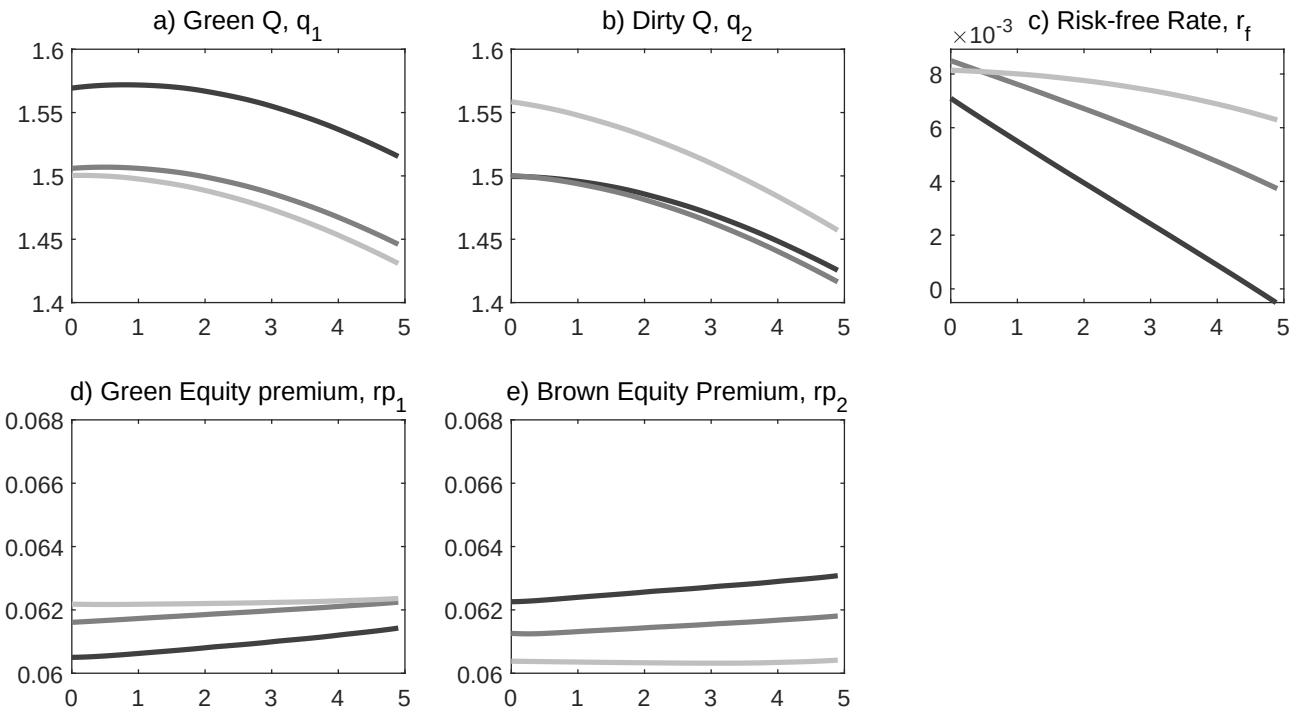

Figure 7: Asset Pricing without Option to Convert. This figure complements Figure 6 and depicts the corresponding results if the option to convert is disregarded. On the horizontal axis is temperature in the range from 0°C to 5°C. The lines represent various levels of the capital share: dark lines (——) depict $S = 0.95$, gray lines (——) refer to $S = 0.5$, and light (——) lines to $S = 0.05$. a) plots Tobin's Q of the green asset, b) shows Tobin's Q of the dirty capital stock, c) depicts the equilibrium risk-free rate, d) shows the risk premium of the green asset, e) depicts the risk premium of the dirty asset.

dirty into green capital at some adjustment costs. If we disregard this option for the moment, then the risk premium of the dirty and green sector is positively related to its share, S and $1 - S$, respectively, which is qualitatively similar to Cochrane et al. (2007). There is hardly any temperature dependence, which can be explained by the deterministic structure of climate damages. This can be seen in Panels d) and e) of Figure 7 which are analogous to Panels d) and e) of Figure 6, but in a framework without the option to convert. Notice that the Tobin's Qs and the risk-free rate are very similar in Figures 6 and 7. We emphasize that when the share of dirty capital in the economy is high, the dirty asset pays a slightly higher risk premium than the green asset. The difference between the risk premia of the two assets is about 0.2% and referred to as a *carbon premium*.

If we also take the option to convert dirty capital into account, the value of the dirty asset involves the value of this option. For economies with high shares of dirty capital and currently

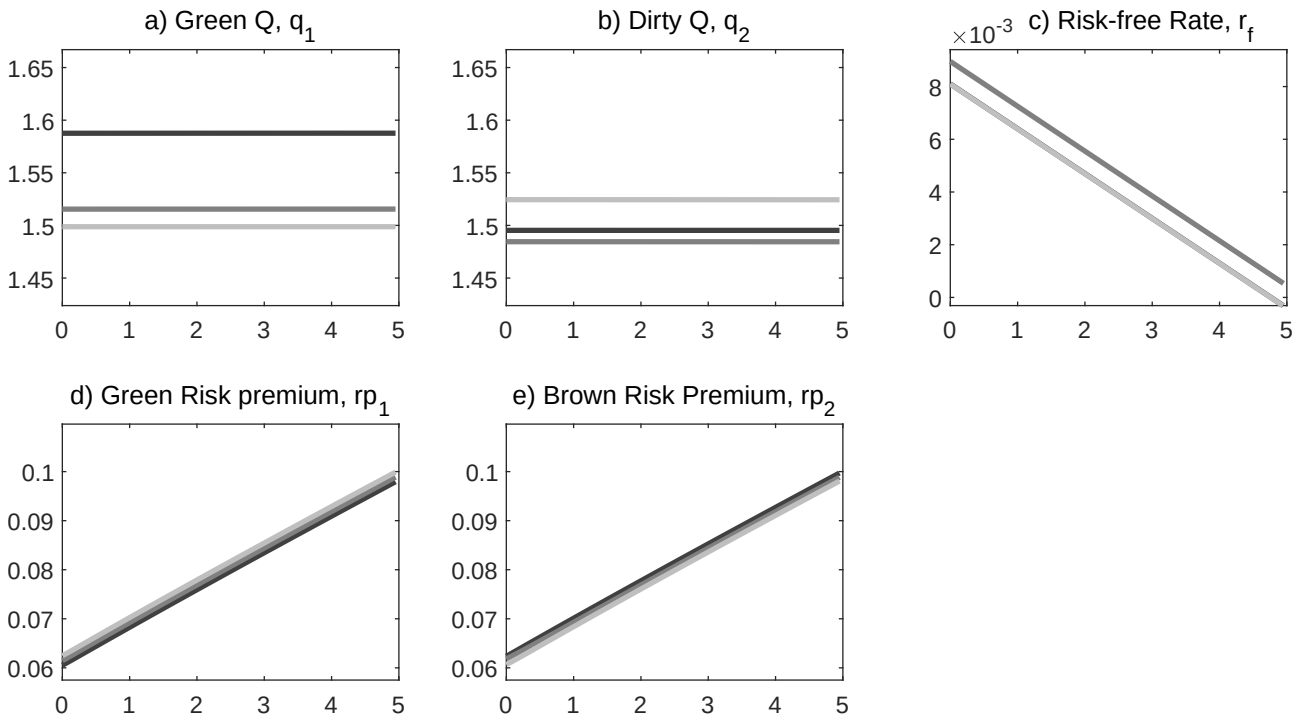

Figure 8: Asset Pricing versus Temperature and the Share of Dirty Capital (Climate Disasters). On the horizontal axis is temperature in the range from 0°C to 5°C. The lines represent various levels of the capital share: dark lines (—) depict $S = 0.95$, gray lines (—) refer to $S = 0.5$, and light (—) lines to $S = 0.05$. a) plots Tobin's Q of the green asset, b) shows Tobin's Q of the dirty capital stock, c) depicts the equilibrium risk-free rate, d) shows the risk premium of the green asset, e) depicts the risk premium of the dirty asset. The option to convert dirty capital into green capital generates interesting qualitative effects but the quantitative implications are modereate.

low temperatures, the option value is relatively high and thus the risk premium of the dirty asset is reduced. This can be seen in Panel e) of Figure 6 where the dark line (—) is now below the gray line (—). However, if the share of dirty capital is small, $S = 0.05$, the diversification motive dominates the value of the option and the premium is even lower (light line (—)).[20]

Furthermore, compared to a model without the option to convert, the existence of this option fully reverses the order of the green risk premium in Panel d). This is because the dirty and clean assets are priced in general equilibrium, i.e., changes in the valuation of the dirty asset also feeds back into the valuation of the green asset.

[20]Notice that the diversification motive is also present in Cochrane et al. (2007).

Results for the Damage Calibration with Climate Disasters Figure 8 depicts the asset pricing implications for the jump impact. Since the disaster intensity grows linearly in temperature, this linearity carries over to the relevant asset pricing quantities. Most of the qualitative results obtained by the moderate damage specification persist for the jump impact. In particular, there is also a carbon risk premium as in the previous paragraph. The most important finding is that with climate disasters the risk premia are strongly affected by temperature. Notice that, in contrast to the Nordhaus specification, economic damages involve tipping risks that increase with temperature and their magnitudes are modeled by a fat-tailed distribution. This yields another dimension of risk, for which investors want to be compensated.

7 Conclusion

Our main concern has been the interplay between climate action and financial considerations. Since agents want to hold diversified asset holdings, the transition towards a low-carbon economy is affected by diversification motives. Diversification and climate action are initially complementary goals, since agents want to decarbonize the economy and hold a balanced portfolio of carbon-free and carbon-intensive assets. At a certain point, however, the two goals become conflicting and a trade-off arises. This is because environmental considerations incentivize the economy to further reduce the dirty capital share, but in turn assets holdings become less diversified. Hence, climate policy is frustrated by the need to diversify financial asset holdings. Furthermore, it is usually not optimal to fully close down carbon-intensive sectors as they serve as a hedge in the long run and keeping the carbon-intensive sector open in the short run allows a faster build-up of green assets in the short run. The qualitative implications of these effects hold for two common approaches to model the adverse effects of climate change on economic activity, the depreciation rate of capital and the risk of macroeconomic disasters, respectively. Only if the impact of climate change on economic activity is significantly more pronounced than suggested by DICE, is it optimal to close down the carbon-intensive sector.

We have also analyzed the dynamics of risk premia and the risk-free rate during the transition towards a low-carbon economy. We show that the existence of potential climate disasters is crucial for finding a significant effect of climate change on asset prices. In the absence of climate disasters, the effect of climate change on asset prices is moderate. From the perspective of policy makers, our findings are challenging. Our results suggest that initially policy makers should

be intrinsically motivated to take climate action, simply to reach diversified asset holdings. Only if policy makers want to speed up the process, they must take extra action. Later in the transition process matters change fundamentally. If policy makers wish to incentivize the economy to reduce the carbon-intensive capital stock beyond its fully diversified share, they must counter the effects of diversification.

Further research is needed to obtain empirical evidence on how climate policy affects the return on and prices of financial assets, both in sectors that make substantial use of fossil fuel and others that make more use of renewable energy. In particular, evidence is needed on the covariance of macroeconomic shocks, both normal and macroeconomic and climate disaster shocks, hitting the brown and green sectors to assess how important the asset diversification and hedging arguments are. Finally, future research needs to depart from the socially optimal outcomes for the global economy and consider policy uncertainty and the consequences for stranding of financial assets and the implications for returns and risk premia.[21]

References

Ackerman, F., E. A. Stanton, and R. Bueno, 2013, Epstein-Zin utility in DICE: Is risk aversion irrelevant to climate policy?, *Environmental and Resource Economics* 56, 73–84.

Allen, M. R., D. J. Frame, C. Huntingford, C. D. Jones, J. A. Lowe, M. Meinshausen, and N. Meinshausen, 2009, Warming caused by cumulative carbon emissions towards the trillionth tonne, *Nature* 458, 1163–1166.

Bansal, R., D. Kiku, and M. Ochoa, 2017, Price of long-run temperature shifts in capital markets, *Working Paper,* Duke University.

Bansal, R., D. Kiku, and M. Ochoa, 2019, Climate change and growth risks, *Working Paper,* Duke University.

Bansal, R., and A. Yaron, 2004, Risks for the long run: A potential resolution of asset pricing puzzles, *Journal of Finance* 59, 1481–1509.

Barnett, M., 2020, Climate change and uncertainty: An asset pricing perspective, *Working Paper,* Arizona State University.

[21] A survey of stranded carbon-intensive assets is provided by van der Ploeg and Rezai (2020).

Barnett, M., W. Brock, and L.P. Hansen, 2020, Pricing uncertainty induced by climate change, *Review of Financial Studies* 33, 1024–1066.

Barro, R. J., 2006, Rare disasters and asset markets in the twentieth century, *Quarterly Journal of Economics* 121, 823–866.

Barro, R. J., 2009, Rare disasters, asset prices, and welfare costs, *American Economic Review* 99, 243–264.

Barro, R. J., and T. Jin, 2011, On the size distribution of macroeconomic disasters, *Econometrica* 79, 1567–1589.

Benzoni, L., P. Collin-Dufresne, and R. Goldstein, 2011, Explaining asset pricing puzzles associated with the 1987 market crash, *Journal of Financial Economics* 101, 552–573.

Bolton, P., and M. Kacperczyk, 2020a, Carbon premium around the world, *Imperial College, London* .

Bolton, P., and M. Kacperczyk, 2020b, Do investors care about carbon risk?, *NBER Working Paper* 26968.

Branger, N., H. Kraft, and C. Meinerding, 2016, The dynamics of crises and the equity premium, *Review of Financial Studies* 29, 232–270.

Bretschger, L., and A. Vinogradova, 2019, Best policy response to environmental shocks: building a stochastic framework, *Journal of Environmental Economics and Management* 97, 23–41.

Cai, Y., and T. S. Lontzek, 2019, The social cost of carbon with economic and climate risks, *Journal of Political Economy* 127, 2684–2734.

Cochrane, J. H., 2005, *Asset pricing* (Princeton University Press).

Cochrane, J. H., F. A. Longstaff, and P. Santa-Clara, 2007, Two trees, *Review of Financial Studies* 21, 347–385.

Crost, B., and C. P. Traeger, 2014, Optimal CO_2 mitigation under damage risk valuation, *Nature Climate Change* 4, 631–636.

Daniel, K., R. Litterman, and G. Wagner, 2019, Declining CO_2 price paths, *Proceedings of the National Academy of Sciences of the United States of America* 116, 20886–20891.

Dell, M., B. F. Jones, and B. A. Olken, 2009, Temperature and income: Reconciling new cross-sectional and panel estimates, *American Economic Review* 99, 198–204.

Dell, M., B. F. Jones, and B. A. Olken, 2012, Temperature shocks and economic growth: Evidence from the last half century, *American Economic Journal: Macroeconomics* 4, 66–95.

Dietz, S., C. Gollier, and L. Kessler, 2018, The climate beta, *Journal of Environmental Economics and Management* 87, 258–274.

Dietz, S., and F. Venmans, 2019, Cumulative carbon emissions andeconomic policy: In search of general principles, *Journal of Environmental Economics and Management* 96, 108–129.

Donadelli, M., M. Jueppner, M. Riedel, and C. Schlag, 2017, Temperature shocks and welfare costs, *Journal of Economic Dynamics and Control* 82, 331–355.

Duffie, D., and L. G. Epstein, 1992a, Asset pricing with stochastic differential utility, *Review of Financial Studies* 5, 411–36.

Duffie, D., and L. G. Epstein, 1992b, Stochastic differential utility, *Econometrica* 60, 353–394.

Duffie, D., and C. Skiadas, 1994, Continuous-time asset pricing: A utility gradient approach, *Journal of Mathematical Economics* 23, 107–132.

Epstein, L. G., and S. E. Zin, 1989, Substitution, risk aversion, and the temporal behavior of consumption and asset returns: A theoretical framework, *Econometrica* 57, 937–969.

Golosov, M., J. Hassler, P. Krusell, and A. Tsyvinsky, 2014, Optimal taxes on fossil fuel in general equilibrium, *Econometrica* 82, 41–88.

Hambel, C., H. Kraft, and E. S. Schwartz, 2018, The social cost of carbon in a non-cooperative world, *NBER Working Paper* 24604.

Hassler, J., P. Krusell, C. Olovsson, and M. Reiter, 2020, On the effectiveness of climate policies, *Working Paper,* Stockholm University.

IPCC, 2014, *Fifth Assessment Report of the Intergovernmental Panel on Climate Change* (Cambridge University Press).

Jensen, S., and C. P. Traeger, 2014, Optimal climate change mitigation under long-term growth uncertainty: Stochastic integrated assessment and analytic findings, *European Economic Review* 69, 104–125.

Karydas, C., and A. Xepapadeas, 2019, Climate change financial risks: pricing and portfolio allocation, *Working Paper,* ETH Zurich.

Kreps, D. M., and E. L. Porteus, 1978, Temporal resolution of uncertainty and dynamic choice theory, *Econometrica* 46, 185–200.

Loayza, N. V., E. Olaberra, J. Rigolini, and L Christiaensen, 2012, Natural disasters and growth: going beyond the averages, *World Development* 40, 1317–1336.

Matthews, H. D., N. P. Gillett, P. A. Stott, and K. Zickfeld, 2009, The proportionality of global warming to cumulative carbon emissions, *Nature* 459, 829–832.

Matthews, H. D., K. Zickfeld, R. Knutti, and M. R. Allen, 2018, Focus on cumulative emissions, global carbon budgets and the implications for climate mitigation targets, *Environmental Research Letters* 13, 010201.

Munk, C., and C. Sørensen, 2010, Dynamic asset allocation with stochastic income and interest rates, *Journal of Financial Economics* 96, 433–462.

Nordhaus, W. D., 1991, To slow or not slow: the economics of the greenhouse effect, *Economic Journal* 101, 920–937.

Nordhaus, W. D., 1992, An optimal transition path for controlling greenhouse gases, *Science* 258, 1315–1319.

Nordhaus, W. D., 2017, Revisiting the social cost of carbon, *Proceedings of the National Academy of Sciences* 114, 1518–1523.

Nordhaus, W. D., and P. Sztorc, 2013, DICE 2013R: Introduction and user's manual, *Technical Report,* Yale University.

Pindyck, R. S., and N. Wang, 2013, The economic and policy consequences of catastrophes, *American Economic Journal: Economic Policy* 5, 306–339.

Rezai, A., and F. van der Ploeg, 2016, Intergenerational inequality aversion, growth and the role of damages: Occam's rule for the global carbon tax, *Journal of the Association of Environmental and Resource Economics* 3, 499–522.

Scheffers, B., L. De Meester, T. Bridge, A. Hoffmann, J. Pandolfi, R. Corlett, S. Butchart, P. Pearce-Kelly, K Kovacs, D. Dudgeon1, M. Pacifici, C. Rondinini, W. Foden, T. Martin, C. Mora, D. Bickford, and J. Watson, 2019, The broad footprint of climate change from genes to biomes to people, *Science* 354, 719–732.

Traeger, C., 2019, Ace–analytic climate economy (with temperature and uncertainty), *Working Paper,* University of Oslo.

van den Bijgaart, I., R. Gerlagh, and M. Liski, 2016, International aspects of pollution control, *Journal of Environmental Economics and Management* 77, 75–96.

van den Bremer, T. S., and F. van der Ploeg, 2019, The risk-adjusted carbon price, *Working Paper,* University of Oxford.

van der Ploeg, F., 2018, The safe carbon budget, *Climatic Change* 147, 47–59.

van der Ploeg, F., and A. Rezai, 2019, Simple rules for climate policy and integrated assessment, *Environmental and Resource Economics* 72, 77–108.

van der Ploeg, F., and A. Rezai, 2020, Stranded assets in the transition to a carbon-free economy, *Annual Review of Resource Economics* 12:4, 1–18.

Wachter, J. A., 2013, Can time-varying risk of rare disasters explain aggregate stock market volatility?, *The Journal of Finance* 68, 987–1035.

A The Reduced-Form Value Function

A.1 Reduced-Form Value Function

To solve the Hamilton-Jacobi-Bellman equation (3.1), we first transform it by expressing the decision variables in relative terms and reducing the number of state variables by one. Let $i_n = I_n/K_n$, $f_n = F_n/K_n$, $r = R/K_1$ denote the relative control variables. We express the value

function in terms of time, total capital K, share of dirty capital S, and temperature T (instead of K_1, K_2, and T). The dynamics of the state variables can be written as

$$\begin{aligned}
\mathrm{d}K_1 &= K_{1-}\Big[\Big(i_1 - \frac{1}{2}\phi_1 i_1^2 + r - \frac{1}{2}\kappa r^2 - \delta_1^k\Big)\mathrm{d}t + \sigma_1 \mathrm{d}W_1 - \big(\ell_e \mathrm{d}N_e + \ell_c \mathrm{d}N_c\big)\Big], \\
\mathrm{d}K_2 &= K_{2-}\Big[\Big(i_2 - \frac{1}{2}\phi_2 i_2^2 - r\frac{K_1}{K_2} - \delta_2^k\Big)\mathrm{d}t + \sigma_2\Big(\rho_{12}\mathrm{d}W_1 + \sqrt{1-\rho_{12}^2}\mathrm{d}W_2\Big) - \big(\ell_e \mathrm{d}N_e + \ell_c \mathrm{d}N_c\big)\Big], \\
\mathrm{d}T &= \widehat{\beta} f_2 \mathrm{d}t + \sigma_T(T)\mathrm{d}W_3,
\end{aligned}$$

where $\widehat{\beta} = \beta/K_2$. To shorten the notation, we write $W = (W_1, W_2, W_3)^\top$ and denote the drift of the capital stocks and temperature by μ_{K_i} and μ_T, respectively. Following Cochrane et al. (2007), we define $K = K_1 + K_2$ and $S = K_2/(K_1 + K_2)$.The dynamics of K and S can be calculated using Ito's lemma:

$$\begin{aligned}
\mathrm{d}S &= S(1-S)\Big[\mu_S(i_1, i_2, r, S)\mathrm{d}t + (\sigma_2\rho_{12} - \sigma_1)\mathrm{d}W_1 + \sigma_2\sqrt{1-\rho_{12}^2}\mathrm{d}W_2\Big] \\
\mathrm{d}K &= K_-\Big[\mu_K(i_1, i_2, r, S)\mathrm{d}t + [(1-S)\sigma_1 + S\sigma_2\rho_{12}]\mathrm{d}W_1 + S\sigma_2\sqrt{1-\rho_{12}^2}\mathrm{d}W_2 - \big(\ell_e \mathrm{d}N_e + \ell_c \mathrm{d}N_c\big)\Big].
\end{aligned}$$

where the drifts are given by

$$\begin{aligned}
\mu_S(i_1, i_2, r, S) &= \mu_{K_1} - \mu_{K_2} + S(\sigma_1\sigma_2\rho_{12} - \sigma_2^2) + (1-S)(\sigma_1^2 - \sigma_1\sigma_2\rho_{12}) \\
\mu_K(i_1, i_2, r, S) &= (1-S)\mu_{K_1} + S\mu_{K_2}
\end{aligned}$$

We thus solve a modified HJB equation with finite differences in terms of only two (S, T) instead of three state variables (K_1, K_2, T). The following Proposition summarizes our findings.

Proposition A.1 (Value Function and Optimal Controls)**.** *Suppose $\widehat{\beta} = \widehat{\beta}(t, S, T)$. The value function (2.5) has the form*

$$J(t, K_1, K_2, T) = \frac{1}{1-\gamma}(K_1 + K_2)^{1-\gamma} G\big(t, T, S(K_1, K_2)\big). \tag{A.1}$$

where G satisfies a certain HJB equation which is given in (A.8) below. The optimal reallocation strategy is

$$r = \frac{1}{\kappa}\Big(\frac{G_S}{G_S S + (\gamma - 1)G}\Big) \tag{A.2}$$

and optimal green energy use is

$$f_1 = \Big(\frac{b_1}{\eta_1 A_1 \Lambda_1(T)}\Big)^{\frac{1}{\eta_1 - 1}}.$$

The optimal investment strategies and fossil fuel use follow from the nonlinear equations:

$$\begin{aligned}
&\big[(1-\gamma)G - G_S S\big][1-\phi_1 i_1] \\
&\qquad = \frac{\delta(1-\gamma)G}{(A_1 f_1^{\eta_1}\Lambda_1(T) - i_1 - b_1 f_1)(1-S) + (A_2 f_2^{\eta_2}\Lambda_2(T) - i_2 - b_2 f_2)S} \qquad \text{(A.3)} \\
&\big[(1-\gamma)G + G_S(1-S)\big][1-\phi_2 i_2] \\
&\qquad = \frac{\delta(1-\gamma)G}{(A_1 f_1^{\eta_1}\Lambda_1(T) - i_1 - b_1 f_1)(1-S) + (A_2 f_2^{\eta_2}\Lambda_2(T) - i_2 - b_2 f_2)S} \qquad \text{(A.4)} \\
&\frac{(A_2\eta_2 f_2^{\eta_2 - 1}\Lambda_2(T) - b_2)S\delta(1-\gamma)G}{(A_1 f_1^{\eta_1}\Lambda_1(T) - i_1 - b_1 f_1)(1-S) + S(A_2 f_2^{\eta_2}\Lambda_2(T) - i_2 - b_2 f_2)} \\
&\qquad = -G_T\beta \qquad \text{(A.5)}
\end{aligned}$$

The optimal social cost of carbon is

$$\tau_c = \frac{\vartheta C}{\delta(\gamma - 1)}\frac{G_T}{G}, \qquad \text{(A.6)}$$

where optimal consumption is

$$C = \Big((1-S)[A_1 f_1^{\eta_1}\Lambda_1(T) - i_1 - b_1 f_1] + S[A_2 f_2^{\eta_2}\Lambda_2(T) - i_2 - b_2 f_2]\Big)K. \qquad \text{(A.7)}$$

Proof. Let $i_n = I_n/K_n$, $f_n = F_n/K_n$, $r = R/K_1$ denote the control variables in relative terms. Substituting these relative controls into (3.1) leads to the HJB equation:

$$\begin{aligned}
0 = \sup_{i_1, i_2, f_1, f_2, r} \Big\{ &\delta(1-\gamma)J\log\Big(\frac{A_1 K_1 f_1^{\eta_1}\Lambda_1(T) + A_2 K_2 f_2^{\eta_2}\Lambda_2(T) - i_1 K_1 - i_2 K_2 - b_1 f_1 K_1 - b_2 f_2 K_2}{[(1-\gamma)J]^{\frac{1}{1-\gamma}}}\Big) \\
&+ J_{K_1}K_1\big(i_1 - \frac{1}{2}\phi_1 i_1^2 + r - \frac{1}{2}\kappa r^2 - \delta_1^k\big) + J_{K_2}K_2\big(i_2 - \frac{1}{2}\phi_2 i_2^2 - r\frac{K_1}{K_2} - \delta_2^k\big) \\
&+ \frac{1}{2}J_{K_1K_1}K_1^2\sigma_1^2 + \frac{1}{2}J_{K_2K_2}K_2^2\sigma_2^2 + J_{K_1K_2}K_1K_2\sigma_1\sigma_2\rho_{12} + J_T\beta K_2 f_2 + J_{TT}\frac{1}{2}\sigma_T(T)^2 + \\
&+ \lambda_e\mathbb{E}[J(K_1(1-\ell_e), K_2(1-\ell_e), T) - J] + \lambda_c(T)\mathbb{E}[J(K_1(1-\ell_c), K_2(1-\ell_c), T) - J]\Big\}
\end{aligned}$$

We conjecture that the value function has the form

$$J(K_1, K_2, T) = \frac{1}{1-\gamma}(K_1 + K_2)^{1-\gamma} G\big(T, S(K_1, K_2)\big).$$

The partial derivatives of S are $S_{K_1} = \frac{-S}{K_1+K_2}$, $S_{K_2} = \frac{1-S}{K_1+K_2}$. This specification implies

$$G(T,S) > 0, \qquad G_T(T,S) > 0.$$

The relevant partial derivatives of the value function J are

$$\begin{aligned}
J_{K_1} &= K^{-\gamma} G + \frac{1}{1-\gamma} K^{1-\gamma} G_S \frac{-S}{K}, \\
J_{K_1K_1} &= -\gamma K^{-\gamma-1} G + 2K^{-\gamma} G_S \frac{-S}{K} + \frac{1}{1-\gamma} K^{1-\gamma} \Big[G_{SS} \frac{S^2}{K^2} + 2G_S \frac{S}{K^2} \Big], \\
J_{K_2} &= K^{-\gamma} G + \frac{1}{1-\gamma} K^{1-\gamma} G_S \frac{1-S}{K}, \\
J_{K_2K_2} &= -\gamma K^{-\gamma-1} G + 2K^{-\gamma} G_S \frac{1-S}{K} + \frac{1}{1-\gamma} K^{1-\gamma} \Big[G_{SS} \frac{(1-S)^2}{K^2} - 2G_S \frac{1-S}{K^2} \Big], \\
J_{K_1K_2} &= -\gamma K^{-1-\gamma} G + K^{-\gamma} G_S \frac{1-2S}{K} + \frac{1}{1-\gamma} K^{1-\gamma} \Big[G_{SS} \frac{-(1-S)S}{K^2} + G_S \frac{2S-1}{K^2} \Big], \\
J_T &= \frac{1}{1-\gamma} K^{1-\gamma} G_T.
\end{aligned}$$

Substituting the conjecture and its partial derivatives into the HJB equation leads to the following reduced-form HJB equation

$$\delta G \log(G) = \sup_{i_1, i_2, f_1, f_2, r} \Big\{ G_t + M_1 G + M_2 G_S + M_3 G_{SS} + M_4 G_T + M_5 G_{TT} \Big\} \tag{A.8}$$

where $\mu_1 = \mu_1(i_1, r, T)$ and $\mu_2 = \mu_2(i_2, r, T, S)$ denote the drifts of the green and brown capital stocks, respectively. Furthermore, we introduce the three-dimensional volatility vectors

$$\sigma_k(S) = \big((1-S)\sigma_1 + S\sigma_2\rho_{12},\, S\sigma_2\sqrt{1-\rho_{12}^2},\, 0 \big)^\top, \tag{A.9}$$

$$\sigma_s = \big(\sigma_2\rho_{12} - \sigma_1,\, \sigma_2\sqrt{1-\rho_{12}^2},\, 0 \big)^\top. \tag{A.10}$$

The coefficients M_ℓ ($\ell = 1, \ldots, 5$) are given by

$$\begin{aligned}
M_1 &= (1-\gamma)\Big[\underbrace{(1-S)\mu_1 + S\mu_2}_{=\mu_k} - \frac{1}{2}\gamma[\underbrace{(1-S)^2\sigma_1^2 + S^2\sigma_2^2 + 2S(1-S)\sigma_1\sigma_2\rho_{12}}_{=\|\sigma_k\|^2}]\Big] \\
&\quad + \lambda_e \mathbb{E}[(1-\ell_e)^{1-\gamma} - 1] + \lambda_c(T)\mathbb{E}[(1-\ell_c)^{1-\gamma} - 1] + \delta(1-\gamma)\log(C/K) \\
M_2 &= S(1-S)\Big(\mu_2 - \mu_1 - \gamma\big[\underbrace{S\sigma_2^2 - (1-S)\sigma_1^2 + (1-2S)\sigma_1\sigma_2\rho_{12}}_{=\sigma_k^\top \sigma_s}\big]\Big) \\
M_3 &= \frac{1}{2}(1-S)^2 S^2\big[\underbrace{\sigma_1^2 + \sigma_2^2 - 2\sigma_1\sigma_2\rho_{12}}_{=\|\sigma_s\|^2}\big] \\
M_4 &= \widehat{\beta} f_2 \\
M_5 &= \frac{1}{2}\sigma_T(T)^2
\end{aligned}$$

where C/K is given in (A.7) and $\widehat{\beta} = \beta/K_2$. The separation thus holds if and only if $\widehat{\beta}$ is independent of K_1 and K_2, i.e., $\widehat{\beta} = \widehat{\beta}(t, T, S)$. Calculating the first-order optimality conditions leads to the nonlinear system of equations (A.2)-(A.5) that determines the optimal controls. Finally, q_1 and q_2 satisfy

$$q_1 = \frac{C}{K}\frac{G - \frac{1}{1-\gamma}G_S S}{\delta G}, \qquad q_2 = \frac{C}{K}\frac{G + \frac{1}{1-\gamma}G_S(1-S)}{\delta G}.$$

This proves the proposition. □

B Stochastic Discount Factor and Asset Prices

B.1 Proof of Proposition 6.1

Duffie and Epstein (1992a) and Duffie and Skiadas (1994) show that the dynamics of the pricing kernel H are given by (6.2) where the relevant partial derivatives of the aggregator are

$$f_c(C, J) = \frac{\delta(1-\gamma)GK^{1-\gamma}}{C}, \qquad f_J(C, J) = \delta(1-\gamma)\Big(\log\Big(\frac{C}{K}\Big) - \frac{1}{1-\gamma}\log G\Big) - \delta.$$

To calculate the dynamics of the SDF, we first compute

$$\frac{\mathrm{d}K^{-\gamma}}{K^{-\gamma}} = \Big(-\gamma\mu_k(i_1, i_2, r, S) + \frac{1}{2}\gamma(\gamma+1)\|\sigma_k\|^2\Big)\mathrm{d}t - \gamma\sigma_k^\top \mathrm{d}W + \sum_{i\in\{e,c\}} \big((1-\ell_i)^{-\gamma} - 1\big)\mathrm{d}N_i.$$

According to Ito's lemma, G satisfies

$$\mathrm{d}G = G[\mu_g \mathrm{d}t + \sigma_g^\top \mathrm{d}W]$$

with

$$\begin{aligned}\mu_g &= \frac{1}{G}\Big(G_t + G_S S(1-S)\mu_s + G_T\beta f_2 + \frac{1}{2}G_{SS}S^2(1-S)^2\|\sigma_s\|^2 + \frac{1}{2}G_{TT}\sigma_T(T)^2\Big),\\ \sigma_g &= \frac{1}{G}\Big(G_S S(1-S)(-\sigma_1 + \sigma_2\rho_{12}),\ G_S S(1-S)\sigma_2\sqrt{1-\rho_{12}^2},\ G_T\sigma_T(T)\Big)^\top. \end{aligned} \tag{B.1}$$

Therefore, by Ito's product rule,

$$\begin{aligned}\frac{\mathrm{d}(GK^{-\gamma})}{GK^{-\gamma}} = &\Big(-\gamma\mu_k(i_1, i_2, r, S) + \frac{1}{2}\gamma(\gamma+1)\|\sigma_k\|^2\Big)\mathrm{d}t + \Big(\mu_g - \gamma\langle\sigma_k, \sigma_s\rangle\frac{G_S}{G}S(1-S)\Big)\mathrm{d}t\\ &+ (\sigma_g^\top - \gamma\sigma_k^\top)\mathrm{d}W + \sum_{i\in\{e,c\}} \big((1-\ell_i)^{-\gamma} - 1\big)\mathrm{d}N_i.\end{aligned}$$

Notice that according to (A.8), this expression can be simplified to

$$\begin{aligned}\frac{\mathrm{d}(GK^{-\gamma})}{GK^{-\gamma}} = &\Big[-\mu_k + \gamma\|\sigma_k\|^2 - \sum_{i\in\{e,c\}} \lambda_i(T)\mathbb{E}[(1-\ell_i)^{1-\gamma} - 1] - \delta(1-\gamma)\log\chi + \delta\log G\Big]\mathrm{d}t\\ &+ (\sigma_g^\top - \gamma\sigma_k^\top)\mathrm{d}W + \sum_{i\in\{e,c\}} \big((1-\ell_i)^{-\gamma} - 1\big)\mathrm{d}N_i.\end{aligned}$$

The capital-consumption ratio $\chi = K/C^*$ has the following dynamics

$$\mathrm{d}\chi = \chi[\mu_\chi \mathrm{d}t + \sigma_\chi^\top \mathrm{d}W]$$

for auxiliary functions $\mu_\chi(t, S, T)$ and $\sigma_\chi(t, S, T)$ to be determined, see Appendix C.2. Then, the dynamics of f_c are given by

$$\frac{\mathrm{d}f_c}{f_c} = \Big[-\mu_k + \gamma\|\sigma_k\|^2 - \sum_{i\in\{e,c\}} \lambda_i(T)\mathbb{E}[(1-\ell_i)^{1-\gamma} - 1] - \delta(1-\gamma)\log\chi + \delta\log G + \mu_\chi\Big]\mathrm{d}t$$

$$+\langle\sigma_g-\gamma\sigma_k,\sigma_\chi\rangle\mathrm{d}t+(\sigma_g^\top-\gamma\sigma_k^\top+\sigma_\chi^\top)\mathrm{d}W+\sum_{i\in\{e,c\}}\big((1-\ell_i)^{-\gamma}-1\big)\mathrm{d}N_i$$

Consequently, the pricing kernel has the following dynamics

$$\begin{aligned}\frac{\mathrm{d}H}{H}&=\big[-\delta-\mu_k+\gamma\|\sigma_k\|^2+\sum_{i\in\{e,c\}}\lambda_i(T)\mathbb{E}[\ell_i(1-\ell_i)^{-\gamma}]\big]\mathrm{d}t+\big[\mu_\chi+\langle\sigma_g-\gamma\sigma_k,\sigma_\chi\rangle\big]\mathrm{d}t \qquad \text{(B.2)}\\&+(\sigma_g^\top-\gamma\sigma_k^\top+\sigma_\chi^\top)\mathrm{d}W+\sum_{i\in\{e,c\}}\big((1-\ell_i)^{-\gamma}-1\big)\mathrm{d}N_i-\lambda(T)\mathbb{E}[(1-\ell)^{-\gamma}-1]\big]\mathrm{d}t.\end{aligned}$$

An application of Itô's lemma gives the drift and volatility vector of optimal consumption as

$$\mu_c(t,S,T)=\mu_k(S)-\mu_\chi(t,S,T)+\|\sigma_\chi(t,S,T)\|^2-\langle\sigma_\chi(t,S,T),\sigma_k(S)\rangle, \qquad \text{(B.3)}$$

$$\sigma_c(t,S,T)=\sigma_k(S)-\sigma_\chi(t,S,T). \qquad \text{(B.4)}$$

Substituting (B.3) and (B.4) into (B.2) and some algebra finishes the proof. □

B.2 Dividend Dynamics

Dividends of asset n are

$$D_n=Y_n-I_n-b_nF_n=\big[A_nf_n^{\eta_n}\Lambda_n(T)-i_n-b_nf_n\big]K_n,\qquad n=1,2.$$

It follows from Proposition A.1 that the term in the square brackets only depends on t, S, and T, but not on K_1 or K_2. Consequently, we can write dividends as

$$D_n=\delta_n(t,S,T)K_n \qquad \text{(B.5)}$$

for functions δ_n that can be determined numerically using the approach described in Appendix C.1. Notice that in equilibrium, the state variables S and T are continuous processes. In turn, the δ_n are continuous functions and follow the dynamics

$$\mathrm{d}\delta_n=\delta_n(\mu_{\delta_n}\mathrm{d}t+\sigma_{\delta_n}^\top\mathrm{d}W)$$

where subscripts of δ_n denote partial derivatives and where drift and volatility are given by

$$\mu_{\delta_n} = \frac{1}{\delta_n}\big[\delta_{n,t} + \delta_{n,S}S(1-S)\mu_S + \delta_{n,T}\mu_T + \frac{1}{2}\delta_{n,TT}\|\sigma_T\|^2 + \frac{1}{2}\delta_{n,SS}S^2(1-S)^2\|\sigma_S\|^2\big],$$
$$\sigma_{\delta_n} = \frac{1}{\delta_n}\big[\delta_{n,T}\sigma_T + \delta_{n,S}S(1-S)\sigma_S\big].$$

An application of Itô's product rule to (B.5) yields the dividend dynamics

$$\mathrm{d}D_i = D_{n-}\Big[\mu_{D_n}\mathrm{d}t + \sigma_{D_n}^\top \mathrm{d}W - \sum_{i\in\{c,e\}} \ell_i \mathrm{d}N_i\Big] \tag{B.6}$$

with

$$\mu_{D_n} = \mu_{K_n} + \mu_{\delta_n} + \sigma_{\delta_n}^\top \sigma_{K_n} \qquad \text{and} \qquad \sigma_{D_n} = \sigma_{K_n} + \sigma_{\delta_n}.$$

In a second step, we determine the dynamics of discounted dividends, $\widehat{D}_i = HD_i$. Another application of Itô's product rule implies

$$\begin{aligned}\mathrm{d}\widehat{D}_n &= D_{n-}\mathrm{d}H + H_-\mathrm{d}D_n + \mathrm{d}\langle D_n^c, H^c\rangle + \Delta D_n \Delta H \\ &= \widehat{D}_{n-}\Big[\mu_{\widehat{D}_n}(S,T)\mathrm{d}t + \sigma_{\widehat{D}_n}(T,S)^\top \mathrm{d}W + \sum_{i\in\{c,e\}} \big((1-\ell_i)^{1-\gamma} - 1\big)\mathrm{d}N_i\Big]\end{aligned}$$

with

$$\mu_{\widehat{D}_n} = \mu_H + \mu_{D_n} + \Theta_H^\top \sigma_{D_n} \qquad \text{and} \qquad \sigma_{\widehat{D}_n} = \Theta_H + \sigma_{D_n}.$$

B.3 Price-dividend Ratios of Dividend Claims

Let $\omega_n = \log\left(\frac{P_n}{D_n}\right)$ denote the log price-dividend ratio of asset n. Due to the representation (B.5) of the dividends, the dynamics of K_n, and the pricing equation (6.4), the price is linear in K_n and thus the price-dividend ratio is independent of K_n. Therefore, it is a continuous process with dynamics

$$\begin{aligned}\mathrm{d}\omega_n &= \omega_{n,t}\mathrm{d}t + \omega_{n,S}\mathrm{d}S + \omega_{n,T}\mathrm{d}T + \frac{1}{2}\omega_{n,TT}\|\sigma_T\|^2\mathrm{d}t + \frac{1}{2}\omega_{n,SS}S^2(1-S)^2\|\sigma_S\|^2\mathrm{d}t \\ &= \omega_n(\mu_{\omega_n}\mathrm{d}t + \sigma_{\omega_n}^\top \mathrm{d}W)\end{aligned}$$

where the drift and the volatility vector are given by

$$\mu_{\omega_n} = \frac{1}{\omega_i}\big[\omega_{n,t} + \omega_{n,S}S(1-S)\mu_S + \omega_{n,T}\mu_T + \frac{1}{2}\omega_{n,TT}\|\sigma_T\|^2 + \frac{1}{2}\omega_{n,SS}S^2(1-S)^2\|\sigma_S\|^2\big]$$
$$\sigma_{\omega_n} = \frac{1}{\omega_i}\big[\omega_{n,T}\sigma_T + \omega_{n,S}S(1-S)\sigma_S\big].$$

In particular, the price-dividend ratio $\mathrm{e}^{\omega_n} = \frac{P_n}{D_n}$ satisfies the following dynamics

$$\mathrm{d}(\mathrm{e}^{\omega_n}) = \mathrm{e}^{\omega_n}\omega_n\Big[\big(\mu_{\omega_n} + \frac{1}{2}\|\sigma_{\omega_n}\|^2\big)\mathrm{d}t + \sigma_{\omega_n}^\top \mathrm{d}W\Big].$$

We rewrite the discounted asset price HP_n as $F_n(\widehat{D}_n, \omega_n) = \widehat{D}_n\mathrm{e}^{\omega_n}$. An application of the Feynman-Kač Theorem yields

$$\mathcal{L}F_n + \mathrm{e}^{-\omega_n}F_n = 0, \tag{B.7}$$

where $\mathcal{L}F_n$ denotes the infinitesimal generator. It follows from Itô's lemma that

$$\frac{\mathrm{d}F_n}{F_{n-}} = \big(\mu_H + \mu_{D_n} + \mu_{\omega_n} + \frac{1}{2}\|\sigma_{\omega_n}\|^2 + \sigma_{\omega_n}^\top\Theta_H + \sigma_{\omega_n}^\top\sigma_{D_n} + \Theta_H^\top\sigma_{D_n}\big)\mathrm{d}t + (\sigma_{\omega_n} + \sigma_{D_n} + \Theta_H)^\top\mathrm{d}W$$
$$+ \sum_{i\in\{c,e\}}\big((1-\ell_i)^{1-\gamma} - 1\big)\mathrm{d}N_i\big].$$

The no-arbitrage condition implies

$$\frac{\mathrm{d}F_n}{F_{n-}} = \mu_H + \mu_{D_n} + \mu_{\omega_n} + \frac{1}{2}\|\sigma_{\omega_n}\|^2 + \sigma_{\omega_n}^\top\Theta_H + \sigma_{\omega_n}^\top\sigma_{D_n} + \Theta_H^\top\sigma_{D_n} + \sum_{i\in\{c,e\}}\lambda_i(T)\mathbb{E}\big[(1-\ell_i)^{1-\gamma} - 1\big]. \tag{B.8}$$

Substituting (B.8) into (B.7) yields

$$0 = \mu_H + \mu_{D_n} + \mu_{\omega_n} + \frac{1}{2}\|\sigma_{\omega_n}\|^2 + \sigma_{\omega_n}^\top\Theta_H + \sigma_{\omega_n}^\top\sigma_{D_n} + \Theta_H^\top\sigma_{D_n} + \sum_{i\in\{c,e\}}\lambda_i(T)\mathbb{E}\big[(1-\ell_i)^{1-\gamma} - 1\big] + \mathrm{e}^{-\omega_n}.$$

Consequently, we end up with the following partial differential equation for ω_n:

$$0 = \mu_H + \mu_{D_n} + \Theta_H^\top\sigma_{D_n} + \mathrm{e}^{-\omega_n} + \omega_{n,t} + \omega_{n,S}S(1-S)\mu_S + \omega_{n,T}\mu_T + \frac{1}{2}(\omega_{n,TT} + \omega_{n,T}^2)\|\sigma_T\|^2$$
$$+ \frac{1}{2}(\omega_{n,SS} + \omega_{n,S}^2)S^2(1-S)^2\|\sigma_S\|^2 + \big(\omega_{n,T}\sigma_T + \omega_{n,S}S(1-S)\sigma_S\big)^\top\Theta_H$$

$$+ \left(\omega_{n,T}\sigma_T + \omega_{n,S}S(1-S)\sigma_S\right)^\top \sigma_{D_n} + \sum_{i\in\{c,e\}} \lambda_i(T)\mathbb{E}\left[(1-\ell_i)^{1-\gamma} - 1\right]$$

Notice that this PDE is nonlinear as it involves squared partial derivatives of ω_n. To simplify the numerical solution approach, we transform this PDE into a linear, parabolic PDE that can be solved with a similar approach as described in Appendix C.1. We substitute $\Omega_n = \mathrm{e}^{\omega_n}$ and end up with

$$\begin{aligned} 0 = 1 &+ \Omega_n\Big(\mu_H + \mu_{D_n} + \Theta_H^\top\sigma_{D_n} + \sum_{i\in\{c,e\}} \lambda_i(T)\mathbb{E}\left[(1-\ell_i)^{1-\gamma} - 1\right]\Big) + \Omega_{n,t} + \Omega_{n,S}S(1-S)\mu_S \\ &+ \Omega_{n,T} + \mu_T\frac{1}{2}\Omega_{n,TT}\|\sigma_T\|^2 + \frac{1}{2}\Omega_{n,SS}S^2(1-S)^2\|\sigma_S\|^2 \\ &+ (\Omega_{n,T}\sigma_T + \Omega_{n,S}S(1-S)\sigma_S)^\top(\Theta_H + \sigma_{D_n}) \end{aligned} \tag{B.9}$$

B.4 Risk Premia

The dynamics of the asset price $P_n = \mathrm{e}^{\omega_n}D_n$ follow via Itô's lemma. We obtain the following asset price dynamics

$$\frac{\mathrm{d}P_n}{P_n} = \mu_{P_n}\mathrm{d}t + \sigma_{P_n}^\top \mathrm{d}W - \sum_{i\in\{c,e\}} \ell_i \mathrm{d}N_i + \sum_{i\in\{c,e\}} \lambda_i(T)\mathbb{E}[\ell_i]\mathrm{d}t$$

where the expected stock return and the volatility vector are given by

$$\begin{aligned} \mu_{P_n} &= \mu_{\omega_n} + \mu_{K_n} + \mu_{\delta_n} + \sigma_{\delta_n}^\top\sigma_{K_n} + \sigma_{K_n}^\top\sigma_{\omega^i} + \sigma_{\delta_n}^\top\sigma_{\omega^i} + \frac{1}{2}\|\sigma_{\omega_n}\|^2 - \sum_{i\in\{c,e\}} \lambda_i(T)\mathbb{E}[\ell_i] \\ \sigma_{P_n} &= \sigma_{\omega_n} + \sigma_{K_n} + \sigma_{\delta_n} \end{aligned}$$

Now, the risk premium of asset n can be computed as the sum of its expected stock return, μ_{P_n}, and its dividend yield, $\mathrm{e}^{-\omega_n}$, minus the risk-free interest rate, r^f, i.e.,

$$\mathrm{rp}_n = \mu_{P_n} + \mathrm{e}^{-\omega_n} - r^f.$$

C Numerical Solution Approach

C.1 Value Function and Optimal Controls

Basic idea We face a problem with an infinite time horizon. Since the boundary conditions on G are unknown, we transform the problem into a similar one with a finite time horizon denoted by $t_{\max}$. In our implementation, we consider a model with a finite time horizon and set $G(t_{\max}, T, S) = 1$, which can be interpreted as that the economy consumes the whole capital stock at $t_{\max}$. Starting with this terminal condition, we work backwards through the time grid until the differences between the value function in $t+1$ and t become negligibly small and the solution converges to that of an infinite time horizon.

Definition of the grid We use a grid-based solution approach to solve the non-linear PDE. We discretize the (t, T, S)-space using an equally-spaced lattice. Its grid points are defined by

$$\big\{(t_n, T_i, S_j) \mid n = 0, \cdots, N_t,\, i = 0, \cdots, N_T,\, j = 0, \cdots, N_S\big\},$$

where $t_n = n\Delta_t$, $T_i = i\Delta_T$, and $S_j = j\Delta_S$ for some fixed grid size parameters Δ_t, Δ_T, and Δ_S that denote the distances between two grid points. The numerical results are based on a choice of $N_T = 200$, $N_S = 600$ and 1 time step per year. Our results hardly change if we use a finer grid or more time steps per year. In the sequel, $G_{n,i,j}$ denotes the approximated value function at the grid point (t_n, T_i, S_j) and $\pi_{n,i,j}$ refers to the corresponding set of optimal controls. We apply an implicit finite-difference scheme.

Finite differences approach In this paragraph, we describe the numerical solution approach in more detail. We adapt the numerical solution approach used by Munk and Sørensen (2010). The numerical procedure works as follows. At any point in time, we make a conjecture for the optimal abatement policy $\pi^*_{n,i,j}$. A good guess is the value at the previous grid point since the abatement strategy varies only slightly over a small time interval, i.e., we set $\pi_{n-1,i,j} = \pi^*_{n,i,j}$. Substituting this guess into the HJB equation yields a semi-linear PDE:

$$0 = -\delta \log(G)G + M_1 G + M_2 G_T + M_3 G_{TT} + M_4 G_S + M_5 G_{SS}$$

with state-dependent coefficients $M_i = M_i(t, T, S)$ as stated in Appendix A. Due to the implicit approach, we approximate the time derivative by forward finite differences. In the approximation, we use the so-called 'up-wind' scheme that stabilizes the finite differences approach. Therefore, the relevant finite differences at the grid point (n, i, j) are given by

$$\begin{aligned}
\mathrm{D}_T^+ G_{n,i,j} &= \frac{G_{n,i+1,j} - G_{n,i,j}}{\Delta_T}, \qquad \mathrm{D}_T^- G_{n,i,j} = \frac{G_{n,i,j} - G_{n,i-1,j}}{\Delta_T}, \\
\mathrm{D}_S^+ G_{n,i,j} &= \frac{G_{n,i,j+1} - G_{n,i,j}}{\Delta_S}, \qquad \mathrm{D}_S^- G_{n,i,j} = \frac{G_{n,i,j} - G_{n,i,j-1}}{\Delta_S}, \\
\mathrm{D}_{TT}^2 G_{n,i,j} &= \frac{G_{n,i+1,j} - 2G_{n,i,j} + G_{n,i-1,j}}{\Delta_T^2}, \qquad \mathrm{D}_{SS}^2 G_{n,i,j} = \frac{G_{n,i,j+1} - 2G_{n,i,j} + G_{n,i,j-1}}{\Delta_S^2} \\
\mathrm{D}_t^+ G_{n,i,j} &= \frac{G_{n+1,i,j} - G_{n,i,j}}{\Delta_t}.
\end{aligned}$$

Substituting these expressions into the PDE above yields the following semi-linear equation for the grid point (t_n, m_i, τ_j)

$$\begin{aligned}
G_{n+1,i,j}\frac{1}{\Delta_t} = G_{n,i,j}\Big[&- M_1 + \frac{1}{\Delta_t} + \mathrm{abs}\Big(\frac{M_2}{\Delta_T}\Big) + \mathrm{abs}\Big(\frac{M_4}{\Delta_S}\Big) + 2\frac{M_3}{\Delta_T^2} + 2\frac{M_5}{\Delta_S^2}\Big] \\
&+ G_{n,i-1,j}\Big[\frac{M_2^-}{\Delta_T} - \frac{M_3}{\Delta_T^2}\Big] + G_{n,i+1,j}\Big[- \frac{M_2^+}{\Delta_T} - \frac{M_3}{\Delta_T^2}\Big] \\
&+ G_{n,i,j-1}\Big[\frac{M_4^-}{\Delta_S} - \frac{M_5}{\Delta_S^2}\Big] + G_{n,i,j+1}\Big[- \frac{M_4^+}{\Delta_S} - \frac{M_5}{\Delta_S^2}\Big] \\
&+ \delta G_{n,i,j}\log(G_{n,i,j})
\end{aligned}$$

Therefore, for a fixed point in time each grid point is determined by a non-linear equation. This results in a non-linear system of $(N_S + 1)(N_T + 1)$ equations that can be solved for the vector

$$G_n = (G_{n,1,1}, \cdots, G_{n,1,N_S}, G_{n,2,1}, \cdots, G_{n,2,N_S}, \cdots, G_{n,N_T,1}, \cdots, G_{n,N_T,N_S}).$$

Using this solution we update our conjecture for the optimal controls at the current point in the time dimension. We apply the first-order conditions and finite difference approximations of the corresponding derivatives. In the interior of the grid, we use centered finite differences. At the boundaries, we apply forward or backward differences.

C.2 Stochastic Discount Factor and Risk Premia

The dynamics of the SDF and the asset prices involve some yet unknown variables. For instance, the risk-free rate (6.3) or the dividend dynamics (B.6) involve the unknown drift and volatility vector of the capital-consumption ratio or the dividend-capital ratio, respectively. These variables depend on the reduced-form value function G in (A.1) and its partial derivatives in a highly nonlinear manner. We thus calculate these variables numerically using finite differences. An application of Itôs lemma to $\chi = \chi(t, S, T)$ implies

$$\mathrm{d}\chi = \chi_t \mathrm{d}t + \chi_S \mathrm{d}S + \chi_T \mathrm{d}T + \frac{1}{2}\chi_{TT}\|\sigma_T\|^2 \mathrm{d}t + \frac{1}{2}\chi_{SS}\|\sigma_S\|^2 \mathrm{d}t$$

where

$$\mu_\chi(t, S, T) = \frac{1}{\chi}\big[\chi_t + \chi_S S(1-S)\mu_S + \chi_T \mu_T + \frac{1}{2}\chi_{TT}\|\sigma_T\|^2 + \frac{1}{2}\chi_{SS}S^2(1-S)^2\|\sigma_S\|^2\big], \quad \text{(C.1)}$$

$$\sigma_\chi(t, S, T) = \frac{1}{\chi}\big[\chi_S S(1-S)\sigma_S + \chi_T \sigma_T\big] \quad \text{(C.2)}$$

Since $\chi = \big((1-S)[A_1 f_1^{\eta_1}\Lambda_1(T) - i_1 - b_1 f_1] + S[A_2 f_2^{\eta_2}\Lambda_2(T) - i_2 - b_2 f_2]\big)^{-1}$ and the optimal controls have already been calculated, we can use finite differences again to determine χ and its partial derivatives. Then, we substitute them into (C.1) and (C.2) to obtain the relavant drift and volatility vector.

D Details on the Calibration

To calibrate the relevant parameters, we follow Pindyck and Wang (2013). Their model only involves a single capital stock and abstracts from climate change, but it is nested by our two-sector model. The model is well-suited to explain *historical* asset returns, since dirty capital has dominated the world economy in the past, but the influence of climate change on asset markets is almost negligible. In the long run, there might be a transition from dirty to green capital. Yet, the current share of green capital is only about 6% indicating that the transition

to green energy has been very modest.[22] We consider the special case of our model with only one capital stock evolving as

$$\mathrm{d}K = \Big(I - \frac{1}{2}\phi\frac{I^2}{K} - \delta_k K\Big)\mathrm{d}t + K\sigma\mathrm{d}W_1 - K\ell_e\mathrm{d}N_e.$$

and output given by $Y = AK^{1-\eta}F^{\eta} = I + C + bF$. In the optimum, the model collapses to a simple AK-technology with linear production function $Y = A^*K$ where productivity is

$$A^* = A\Big(\frac{b}{\eta A}\Big)^{\frac{\eta}{\eta-1}}.$$

The one-sector model is close to that of Pindyck and Wang (2013), but involves energy input F which does not cause climate change. We choose the parameters to generate a real expected growth rate of consumption of $\overline{\mu}_c = 2\%$, an average consumption rate of $\frac{C}{A^*K} = 75\%$ of GDP, a risk-free interest rate starting at $r^f = 0.8\%$, an average risk premium of $\mathrm{rp} = 6.3\%$, and Tobin'Q's of $q = 1.5$. The following equations constitute a non-linear system that relates δ, γ, A^*, ϕ, and δ_K to these quantities

$$\frac{C}{A^*K} = \frac{\phi - A^* + \sqrt{(\phi - A^*)^2 + 4\phi\delta}}{2\phi} \tag{D.1}$$

$$\overline{\mu}_c = -\delta_k K + A\Big(1 - \frac{C}{A^*K} - \eta\Big) - \frac{1}{2}\phi A^2\Big(1 - \frac{C}{A^*K} - \eta\Big)^2 - \frac{\lambda_e}{\alpha_e + 1} \tag{D.2}$$

$$r^f = \delta + \overline{\mu}_c - \frac{1}{2}\sigma_c^2 - \lambda_e\frac{(1-\gamma)(\alpha_e - \gamma) + \gamma(\alpha_e - \gamma + 1)}{(\alpha_e - \gamma)(\alpha_e - \gamma + 1)} + \frac{\lambda_e}{\alpha_e + 1} \tag{D.3}$$

$$\mathrm{ep} = \gamma\sigma_c^2 + \lambda_e\gamma\Big[\frac{1}{\alpha_e - \gamma} - \frac{\alpha_e}{(\alpha_e + 1)(\alpha_e - \gamma + 1)}\Big] \tag{D.4}$$

$$q = \frac{1}{1 - \phi i} \tag{D.5}$$

For the derivation of these equations and for further details, we refer to Pindyck and Wang (2013).

[22] See the website of the UNFCCC. https://unfccc.int/news/green-economy-overtaking-fossil-fuel-industry-ftse-russel-report

E State-Space Solutions

This appendix discusses the influence of the state variables on the optimal decisions and asset returns. From this, we derive intuition for the influence of the share of dirty capital and temperature on the optimal controls and understand the economic forces at play. In particular, we discuss how climate change affects the interest rate and asset returns. All the results are for the benchmark calibration for the year 2100 and for the level impact (L–I). The policy functions behave in a qualitatively similar manner for other years and for our alternative parametrizations of damages. The qualitative behavior of the asset returns is hardly affected by the choice of the damage specification. The lines in Figure E.1 present various levels of the capital share: The dark lines (—) depict $S = 0.95$, the gray lines (—) refers to $S = 0.5$, and the light lines (—) to $S = 0.05$. The horizontal axis depicts the temperature in the range from 0°C to 5°C.

Panel a) of Figure E.1 shows that the optimal investment in the green capital stock decreases in the share of dirty capital S, whereas Panel b) shows that the opposite is true for the investment in the dirty capital stock. This can be explained by the diversification argument from Section 3. If damages are moderate (as for the DICE damage specification), the economy retains a certain level of dirty capital to reach an optimal level of diversification. Therefore, the agent invests more in the green capital stock if the share of dirty capital is high and more in the dirty capital stock if this share is low. Panel c) shows that the optimal consumption strategy hardly depends on the share of dirty capital. This reflects the agent's motive for consumption smoothing. Instead of adjusting the consumption rate in response to the changes in the share of dirty capital, the economy increases the green investment ratio and decreases the dirty investment ratio to smooth consumption. Panel d) depicts fossil fuel use relative to the respective capital stock, which does not vary very much with the share of dirty capital. The corresponding ratio for green energy, F_1/K_1, does not depend on the share of dirty capital at all.[23] Panel e) depicts carbon emissions and shows that in absolute terms fossil fuel use decreases both in the share of dirty capital and temperature.

Panel f) depicts the optimal carbon tax as a fraction of total capital. It shows that the optimal carbon tax sharply increases in temperature and increases only moderately in the share of dirty assets. In recent years, a literature has evolved that derives simple formulas for the optimal social cost of carbon in deterministic environments (e.g., Nordhaus 1991; Golosov et al. 2014, Rezai and van der Ploeg 2016; van den Bijgaart et al. 2016; van der Ploeg and Rezai 2019

[23] See the first-order condition (3.5).

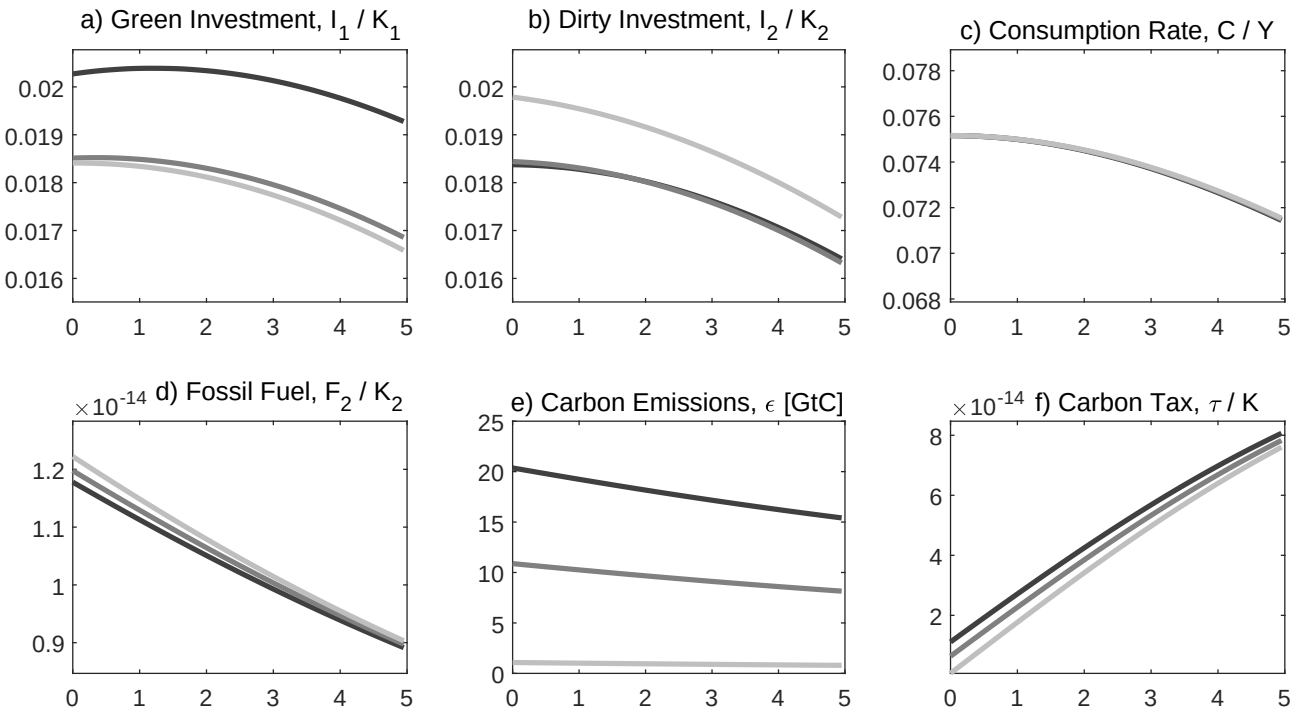

Figure E.1: Policy Functions with only Level Impact (L-I) Global Warming Damages. The graphs depict policy rules for the level impact as functions of the two state variables. On the horizontal axis is temperature in the range from 0°C to 5°C. The lines represent various levels of the capital share: dark lines (——) depict $S = 0.95$, gray lines (——) refer to $S = 0.5$, and light (——) lines to $S = 0.05$. a) plots green investment as a fraction of green capital, b) shows dirty investment as a fraction of dirty capital, c) depicts consumption as a fraction of output, d) shows green energy as a fraction of green capital, e) depicts fossil fuel use as a fraction of dirty capital, and f) shows the optimal carbon tax as a fraction of total capital.

and Hambel et al. 2018). This strand of literature considers analytical models and generates social costs of carbon that do not depend on temperature.[24] By contrast, our framework explicitly models stochastic climate risks and uses a convex damage function, which yields temperature-dependent carbon taxes and optimal controls. Consequently, society reacts to increasing climate risks by raising carbon taxes and thus to more pronounced carbon abatement for higher temperatures. For the damage specification (D–I), damages are linear in temperature

[24]The reason is that the concavity of the logarithmic Arrhenius' law linking temperature to the atmospheric stock of carbon is (more or less) exactly offset by the convexity of the function relating the damage ratio to temperature (Golosov et al. 2014). For more convex damage ratios, the ratio of the optimal SCC to GDP increases in temperature (e.g., Rezai and van der Ploeg 2016).

rather than convex. In turn, the policy functions are almost independent of temperature as in the above mentioned strand of literature.[25]

F Optimal Policy Simulations

Here we present our our optimal policy simulation results over the next 100 years. The columns of Figures F.1 and F.2 show results for the two damage specifications (L–I), and (D–I), respectively. Unless otherwise stated, we use the benchmark calibration summarized in Table 1. Optimal paths are depicted by solid lines (——) and BAU paths by dotted lines (·····). Dashed lines (- - -) show 5% and 95% quantiles of the optimal solution. Appendix E shows the state-space solutions that are used to get these simulations.

F.1 Effects of Climate Policy on the Economy

Figure F.1 depicts the optimal evolution of the real economy under two different damage specifications. It shows that the qualitative behavior is similar for all specifications.

Panels a1)-a2) depict the time paths of output. As a result of climate action, the optimal evolutions exhibit a higher economic growth compared to the BAU evolution since some of the climate damages are avoided. This is true for both damage specifications. For the disaster impact, the climate damages are more pronounced and economic growth is significantly dampened compared to the level impact.

Panels b1)-b2) depict that the consumption-output ratio is in a narrow range between 75% to 76%. Notice that the confidence band of the optimal consumption rate is significantly wider for (L–I) than for (D–I). This is because society responds with a more temperature-sensitive consumption strategy under level impact damages. In particular, for the BAU case, the optimal consumption-output ratio sharply increases for high temperatures around 4°C. A potential explanation is the convexity of the damage function, which leads to a higher sensitivity to atmospheric temperature. For the other damage specification, which is linear in temperature, optimal consumption exhibit small variation across states. In the BAU case, optimal consumption is almost constant.

[25]The corresponding figures are available upon request.

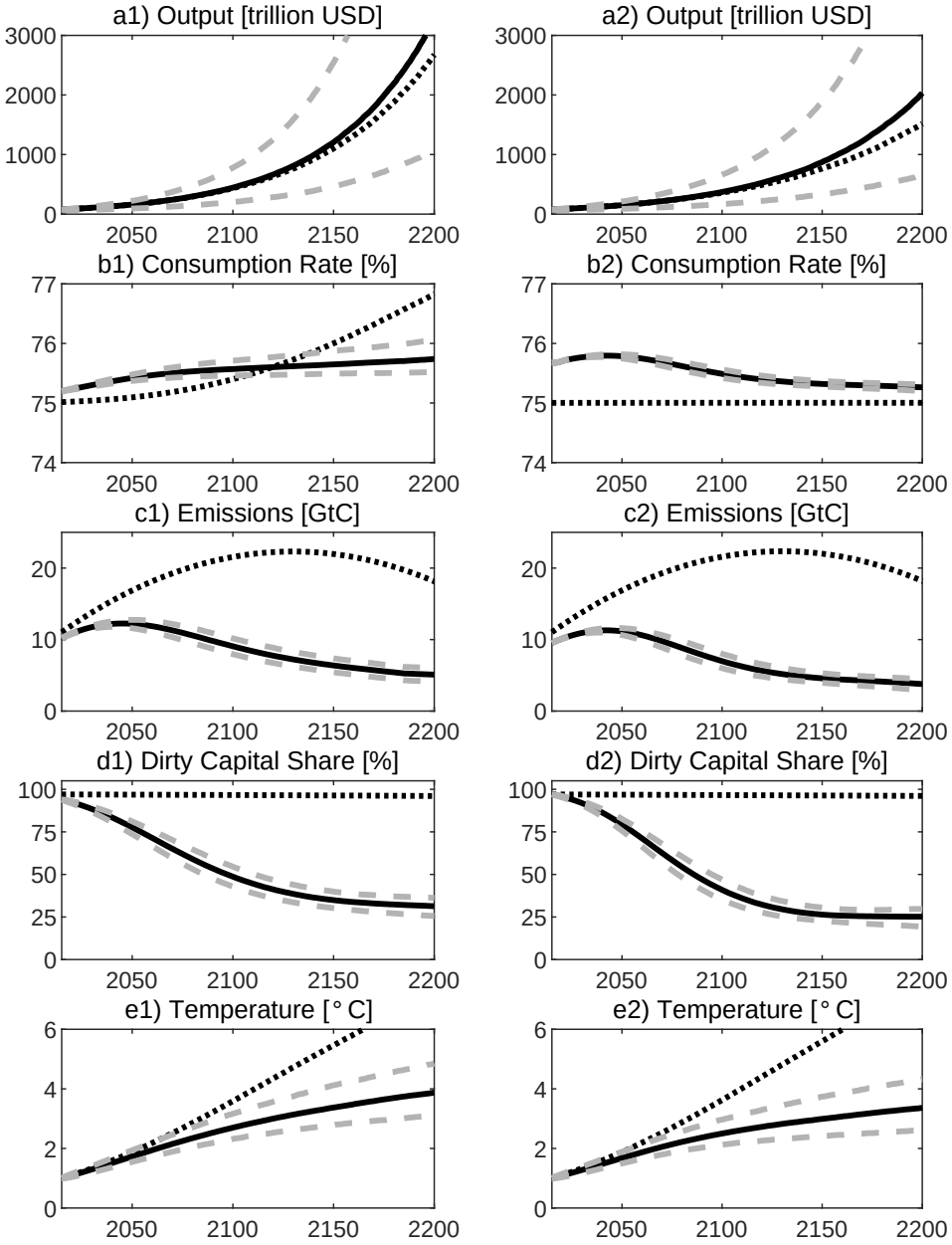

Figure F.1: Evolution of Temperature, the Social Cost of Carbon and the Real Economy. The figure depicts the simulation of the real economy for the two damage specifications level impact (1st column) and disaster impact (2nd column) until the year 2200. Median optimal paths are depicted by solid lines (——) and median BAU paths by dotted lines (·····). Dashed lines (- - -) show 5% and 95% quantiles of the optimal solution. Panels a1)-a2) show the evolution of output. Panels b1)-b2) depict the consumption rate expressed as a fraction of output, i.e., C/Y. Panels c1)-c2) depict the evolution of carbon emissions. Panels d1)-d2) show the evolution of the share of dirty capital S. Panels e1)-e2) depict the evolution of global average temperature increase and Panels f1)-f2) show the optimal carbon tax.

Panels c1)-c2) depict the evolution of the carbon dioxide emissions that are significantly dampened compared to the BAU case. In general, the variation of optimal emissions is low. As discussed in the previous section, optimal emissions are mainly driven by the share of dirty capital, while the influence of temperature is relatively weak. The small variation of the optimal carbon dioxide emissions thus follows from the small variation in S depicted in Panels d1)-d3). The evolution of the share of dirty capital is crucial for understanding the interaction between the diversification and the abatement motive. If we disregard damages from climate change, the share of dirty assets eventually stabilizes at $S^* = 50\%$. On the other hand, if society recognizes climate change and fights global warming, the share of dirty capital decreases to approximately 30%. However, dirty capital does not vanish completely since some positive amount is kept to satisfy the diversification motive. In this sense, the diversification motive eventually reduces climate action. This result is robust across all damage specifications.[26]

F.2 Effects of Climate Policy on Asset Prices

Figure F.2 complements the results presented in Figure F.1 with asset pricing results. Panels a1)-a2) depict the evolution of the green Tobin's Q, whereas Panels b1)-b2) show the evolution of the dirty one. In the optimum, the green Tobin's Q decreases over time, but the dirty Tobin's Q remains always smaller than the green Tobin's Q. For the disaster impact, the green Q stabilize around 1.5, while for the level impact the green Tobin's Q continues to decrease below that level.

Panels c1)-c2) show that the equilibrium risk-free interest rate decreases for all scenarios including BAU, since over time the expected damages from global warming become more pronounced and households respond with higher precautionary savings. This effect is much stronger under BAU, since then climate damages are more severe. In contrast, if carbon is optimally priced, the downward trend of the risk-free interest rate is less pronounced.

Panels d1)-d2) show the evolution of the green risk premium, whereas Panels e1)-e2) depicts the evolution of the dirty risk premium. As discussed, the dirty risk premium depends on the state variables S and T in a non-linear way. This might explain the "snake-shaped" evolution of the dirty risk premium over time for the level impact. For the disaster impact, the risk premiums

[26] If all three damage specifications impact simultaneously, the combined response is more than the sum of the individual policy reactions, and the share of dirty capital eventually goes to zero. The reason is that the more damage global warming does the more likely it is we get into more damaging regions. In other words, the externalities reinforce each other. These results are available upon request.

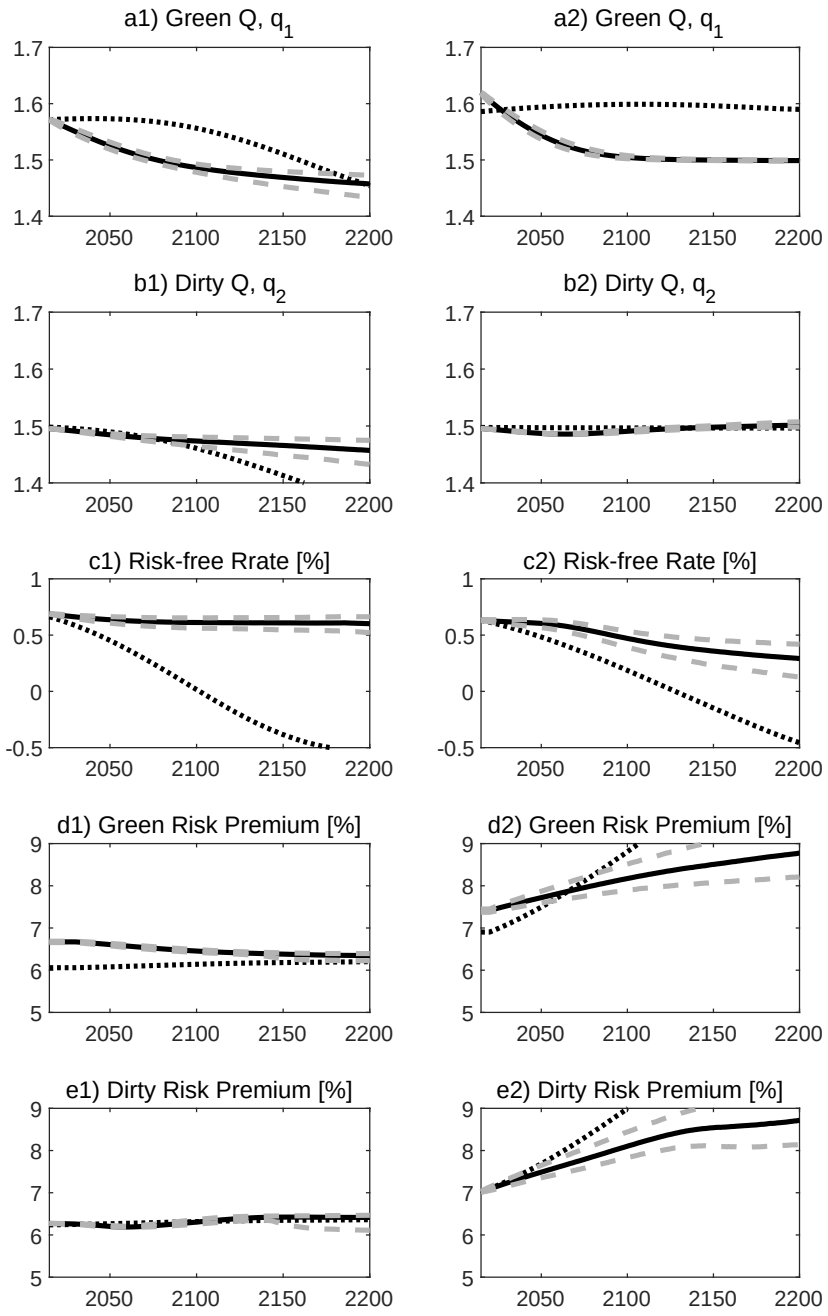

Figure F.2: Evolution of Tobin's Q's, Risk-Free Rates and the Risk Premiums. The figure depicts the simulation of the asset pricing quantities for the two damage specifications level impact (1st column) and disaster impact (2nd column) until the year 2200. Median optimal paths are depicted by solid lines (——) and median BAU paths by dotted lines (·····). Dashed lines (- - -) show 5% and 95% quantiles of the optimal solution. Panels a1)-a2) show the evolution of the Tobin's Q of the green asset and Panels b1)-b2) depict the evolution of the Tobin's Q of the dirty asset. Panels c1)-c2) depict the evolution of the equilibrium risk-free rate. Panels d1)-d2) show the evolution of the risk premium of the green asset. Panels e1)-e2) depict the evolution of the risk premium of the dirty asset.

are higher and increasing. This is triggered by the additional Poisson shock N_e which gives rise to an extra component in the risk premium, as seen in Proposition 6.1. Since the jump intensity increases in temperature and global warming becomes more significant over time, the relative importance of the extra component sharply increases under BAU. This reflects the fact that asset holders must be compensated for the increasing climate risks.